

Atmospheric abundances in post-AGB candidates of intermediate temperature^{*}

A. Arellano Ferro¹, Sunetra Giridhar², P. Mathias³.

¹Instituto de Astronomía, Universidad Nacional Autónoma de México, Apdo. Postal 70-264, México D.F. CP 04510; armando@astroscu.unam.mx

²Indian Institute of Astrophysics, Bangalore 560034, India giridhar@iiap.ernet.in

³ Observatoire de la Côte d'Azur, Département Fresnel, UMR 6528, B.P. 4229, F-06304 Nice Cedex 04, France mathias@obs-nice.fr

Received xxxxx; accepted xxxxx

Abstract. Detailed atmospheric abundances have been calculated for a sample of A-G supergiant stars with IR fluxes and/or high galactic latitudes. HD 172481 and HD 158616 show clear indications of being post-AGB stars that have experienced third dredge-up. HD 158616 is carbon-rich while the abundance pattern of HD 172481 and its large Li enhancement gives support to the hot bottom burning scenario that explains paucity of carbon-rich stars among AGB stars. HD 172324 is very likely a hot post-AGB star that shows a strong carbon deficiency. HD 725, HD 218753 and HD 331319 also appear to be evolved objects between the red giant and the AGB. HD 9167, HD 173638 with a few exceptions, reflect solar abundances and no signs of post red giant evolution. They are most likely young massive disk supergiants. Further analysis of proto-Planetary Nebula HDE 341617 reveals that He lines show signs of velocity stratification. The emission lines have weakened considerably since 1993. The envelope expands at 19 km s⁻¹ relative to the star. Atmospheric abundances, evolutionary tracks and isochrones are used to estimate masses and ages of all stars in the sample.

Key words: Stars: post-AGB; Stars: chemically peculiar; Stars: evolution; Stars: individual HD 725, HD 9167, HD 158616, HD 172324, HD 172481, HD 173638, HD 218753, HD 331319, HDE 341617.

1. Introduction

The atmospheric chemical composition of post-asymptotic giant branch (post-AGB) stars and circumstellar environments is determined by nucleosynthesis and dredge-up events at the late AGB phases. At AGB, the star has a C–O core surrounded by helium and hydrogen burning shells above which lies a deep convective envelope. The thermally pulsating phase (TP-AGB), though much shorter than early AGB phase (E-AGB), is responsible, through considerable mass-loss, for the ejection of large fraction of carbon and *s*-process elements into the ISM. At this phase, thermal pulses are caused by instabilities in the He-burning shell first discovered by Schwarzschild & Härm (1965) and Weigert (1966). The excess energy generated by He shell flashes is transported by convection over the region that extends from the base of He-burning shell and the hydrogen-helium discontinuity. The He shell instabilities strongly influence the chemical composition of the convective envelope. The expansion and cooling of the intershell layers during a powerdown phase of the He shell flash causes the deepening of the convective envelope into regions containing the products of partial He-burning. The ¹²C, ¹⁹F and the *s*-process elements are mixed into the outer envelope causing abundance variations at the surface of these stars. This process, known as the third dredge-up (TDU), is able to explain the formation of carbon stars (Busso, Gallino & Wasserburg 1999), Wallerstein et al. (1997), Mowlavi (1999). At AGB the star is constantly losing mass, but a final phase of enhanced mass-loss by the superwind is believed to terminate the AGB phase producing a planetary nebula. Therefore, studying the chemical composition of the atmospheres and envelopes of evolved stars with IR fluxes, one expects to identify post-AGB stars and to provide important observational constraints

^{*} Based on observations obtained at the Haute-Provence Observatory, France.

for the theoretical work on nucleosynthesis, internal structure and mass-loss in evolved intermediate and low-mass stars.

Post-AGB stars, as they evolve across the H-R diagram towards the white dwarf stage, form families of rather exotic objects like the R CrB stars, other subgroups of H-deficient and He-rich stars, planetary nebulae etc. In the H-R diagram, they populate the region generally occupied by massive young supergiants evolving redwards from the main sequence, and having similar temperatures and luminosities. To differentiate the massive and young stars from the highly evolved low-mass post-AGB stars, detailed atmospheric abundance analysis is crucial.

Chemical analysis of high galactic latitude A-F supergiants have led to the discovery of many interesting post-AGB stars such as HR 7671 (Luck et al. 1990), HR 4912 (Lambert et al. 1983), HR 4114 (Giridhar et al. 1997) or of selected IRAS sources such as IRAS 22223+4327 and IRAS 04296+3429 (Decin et al. 1998). However, most of these high galactic latitude stars are field stars of unknown distances. It is therefore likely that a significant fraction of them could possibly turn out to be disk objects of nearly solar compositions. A search of post-AGB stars among high galactic latitude stars could be more rewarding if we put the additional constraint of IR detection. The wavelength dependence of IR fluxes and also the detection of submillimeter fluxes could give valuable information on the circumstellar matter surrounding the evolved star. The IRAS two colour diagrams such as those published by Olton et al. (1984), van der Veen and Habing (1988) etc., are extremely useful in separating stars with different kinds of envelopes.

In this study, we have undertaken the abundance analysis of a selected sample of stars likely to be post-AGB stars. From the published lists of high galactic latitude stars ($b > 20^\circ$) (e.g. Bidelman 1990 and others) we chose the ones with known infrared fluxes. Among them, the ones falling into the regions VIa and VIb of figure 5b of van der Veen & Habing (1988) were preferred as they were more likely to be post-AGB stars. We have also included a few objects belonging to the regions IIIa and IIIb that are likely to be evolved stars with oxygen-rich envelopes.

The hot star HD 172324 was also included in spite of not being an IRAS source since it has high radial velocity (-110 km s^{-1}) and very complex structures in hydrogen line profiles. It appeared to be a possible hot post-AGB star similar to those investigated by Conlon et al. (1993a;b).

A search for post-AGB stars among supergiant-like stars of high galactic latitude is expected to be more efficient since the possibility of forming stars at truly large distances from the galactic plane is low.

This program is also aimed at providing calibrators for photometric empirical calibrations of atmospheric abundances (Arellano Ferro & Mantegazza 1996), tempera-

tures, and gravities in particular, since gravities are better determined from the ionization equilibrium.

This paper is organized in the following way: Sect. 2 describes the observations and data reduction; Sect. 3 discusses the methodology of abundance calculation; Sect. 4 gives an account of the sources of uncertainty in the derived abundances; in Sect. 5 the results are given and discussed for each star; in Sect. 6 these results are discussed in terms of the evolutionary status of each star while in Sect. 7 we summarize our results.

2. Observations and data reduction

The observational material for this work was obtained during July 6 - July 12, 1999 with the 1.93m telescope of the Haute-Provence Observatory (OHP), which is equipped with the high resolution (42,000) echelle spectrograph ELODIE. Details about the performance and characteristics of the instrument have been thoroughly described by Baranne et al. (1996). We have used one spectrum of HD 172324 taken on June 1995 with the Sandiford echelle spectrograph at 2.1m telescope of McDonald Observatory. This instrument giving a resolution of 50,000 has been described in McCarthy et al. (1993). One spectrum of HD 172481 was obtained with the 2.7m 2dcoudé echelle spectrograph described in Tull et al. (1995). These spectra were reduced using spectroscopic data reduction tasks available in the IRAF package.

2.1. The sample

Table 1 contains the list of stars studied in this work, their spectral types, magnitudes, galactic positions and, when available, the IRAS infrared fluxes.

2.2. Spectroscopic reductions

All spectra were bias-subtracted and flat-field corrected using standard OHP procedures described by Baranne et al. (1996). The spectra were wavelength calibrated with Th-Ar hollow cathode lamp spectra taken after each stellar exposure. More than one exposure was taken and spectra were combined to attain S/N of at least 50. The ELODIE spectrograph gives a resolution of 42,000 and the wavelength coverage goes from 3906 to 6811 Å in 67 echelle orders with some overlaps in adjacent orders.

The equivalent widths were measured using the *spot* task of the IRAF package and their accuracy is generally better than 10% for spectra with S/N ratio larger than 50. We generally restricted ourselves to unblended weak features and avoided using lines stronger than 200 mÅ.

3. Abundance Analysis

We have used ATLAS9 (Kurucz 1993) model atmospheres as an input to the 1997 version of LTE line synthesis program MOOG first described in Sneden (1973). The pro-

Table 1. Basic data and IRAS fluxes of sample stars

Star	Sp.T.	V (<i>mag.</i>)	l ($^{\circ}$)	b ($^{\circ}$)	IRAS	12μ (<i>Jy</i>)	25μ (<i>Jy</i>)	60μ (<i>Jy</i>)	100μ (<i>Jy</i>)
HD 725	F5Ib-II	7.08	117.56	-5.19	00091+5659	.36	.25	.40	14.43
HD 9167	F1III	8.19	127.73	-0.97	01285+6115	.47	.25	.40	8.14
HD 158616	F8	9.69	13.23	+12.17	17279-1119	3.52	2.90	1.60	1.98
HD 172324	B9Ib	8.16	66.18	+18.58					
HD 172481	F2Ia0	9.09	6.72	-10.37	18384-2800	5.41	5.22	.59	1.85
HD 173638	F2Ib-II	5.73	23.38	-3.56	18439-1010	1.41	.39	.67	55.03
HD 218753	A5III	5.69	110.28	-1.02					
HD 331319	F3Ib	9.50	67.16	+2.73	19475+3119	.54	37.99	55.83	14.76
HDE 341617	A5	9.40	50.67	+19.79	18062+2410	3.98	19.62	2.90	1.00

cedure assumes plane-parallel atmospheres, hydrostatic equilibrium and LTE. The oscillator strength or gf value is an important atomic datum that affects the abundance calculations. For elements C, N and O we used gf values from Wiese, Führt & Deters (1996). For Fe I, the values were taken in order of preference from; Table A1 of Lambert et al. (1996), Luck’s compilation (1996; private communication), and Giridhar & Arellano Ferro (1989). For Fe II lines we used the Table A2 of Lambert et al. (1996), Giridhar & Arellano Ferro (1995) and Luck’s compilation (1996; private communication).

For elements other than Fe, the large compilation by Luck (1996; private communication) was preferentially used and for some heavy s -process elements gf values were taken from the work of Thévenin (1989; 1990).

3.1. Determination of atmospheric parameters

In addition to abundances, the line strengths are strongly affected by atmospheric parameters like the effective temperature (T_{eff}), gravity ($\log g$) and turbulent velocity (ξ_t). It is therefore necessary to determine these parameters before using line strengths for abundance determinations.

3.1.1. Effective Temperature

Temperature calibrations exist that are valid for specific spectral type ranges. These methods are not only useful but also complement the spectroscopic efforts by providing initial values for the atmospheric parameters for calculating the atmospheric abundances. Here we briefly describe some of those calibrations that have been used for the stars of our sample. Later in Sect. 5, comparison with the finally adopted spectroscopic results is made in the discussion of each individual star.

Firstly, a rough estimate of T_{eff} can be made from the given spectral type and the calibration of Schmidt-Kaler (1982). However, more accurate values can be obtained from precise photometric colours. For our sample, we have

used $uvby\beta$ photometric data and our own unpublished calibrations for F-G stars (HD 725, HD 9167, HD 172481). In addition, the calibration of Napiwotzki, Schönberner & Wenske (1993) for hotter stars like HD 172324, the 13-colour photometric system and the calibration of Bravo Alfaro et al. (1997), and the Geneva colour indices and the calibration of Cramer & Maeder (1979) were used as appropriate. These empirical calibrations provide T_{eff} with accuracies of ± 500 K or better and serve as excellent starting values that are further refined by spectroscopic approaches. Any drastic difference between the two approaches deserves attention.

Yet another independent approach to estimate T_{eff} is from the Balmer lines profiles fitting (e.g. Arellano Ferro 1985; Venn 1995a). Theoretical Balmer profiles for grids of model atmospheres have been calculated by Kurucz (1993). For stars of intermediate temperature, this method does not lead to unique T_{eff} , but rather it defines loci of possible temperatures and gravities. On the other hand, similar loci can be found from species where two states of ionization are well represented. Again, the solution is not unique but rather a locus on the $T_{\text{eff}} - \log g$ plane is defined for each element. This approach will be illustrated in Fig. 3 for H_{γ} , H_{δ} , Mg and Si for the star HD 218753. The above solution is of special importance for hot stars where no Fe I lines are present. For hotter stars, lines of Fe I are not only very weak but are also influenced by non-LTE effects. For A-F supergiants non-LTE effects could cause errors in the range of 0.2 to 0.3 dex in the iron abundance derived using Fe I lines (Boyarchuck et al. 1985). For example, in the well-known star Vega (A0V), the neglect of departure from LTE for Fe I lines leads to the underestimation of Fe abundance by 0.3 dex (Gigas 1986).

For stars cooler than 7500 K the lines of Fe I and Fe II with wide range in line strengths and lower excitation potential are adequate for estimating the effective temperature, microturbulence and gravity for any given star.

The finally adopted T_{eff} for our stars is that for which abundance consistency is obtained from neutral and ionized lines of well represented species such as Fe, Ti and Cr.

3.1.2. Gravity

A good discussion of atmospheric parameters determination for A type stars can be found in Venn (1995a), who points out that H_γ and H_δ , being very sensitive to temperature and gravity in A type stars, provide a locus of possible temperature-gravity pairs, and that ionisation equilibrium of Mg I and Mg II gives another useful locus of temperature-gravity pair as the non-LTE effects are expected to be very small in magnesium lines. Since ionisation equilibrium of Si I and Si II give a temperature-gravity pair very similar to that given by Mg I and Mg II, the latter can also serve as yet another indicator of these parameters. Intersection of the above mentioned loci could lead to reliable temperature and gravity for each star, as demonstrated in Fig. 3.

The hydrogen lines were distorted in many of the program stars due to underlying emission, and therefore could not be used to derive temperature-gravity loci. We used excitation equilibrium of Fe I lines to get a preliminary estimate of T_{eff} . It was followed by ionisation equilibrium of Mg I/Mg II, Si I/Si II and Cr I/Cr II to arrive at a satisfactory estimate of T_{eff} and $\log g$. For HD 725, HD 9167, HD 158616, HD 172481 and HD 173638 the excitation equilibrium of Fe I lines (requiring derived abundances to be independent of the lower excitation energy of the lines) gave very good estimates of the temperature which were further verified using lines of other species, as mentioned above. Similarly, for gravities, the values giving a good consistency for neutral and ionised Mg, Ti, Cr and Fe were adopted.

The star HD 172324 required an altogether different approach as described in Sect. 5.4.

3.1.3. Microturbulence velocity

All our program stars turned out to be hotter than 7000 K (see Table 2). For hotter stars, Fe I lines were difficult to measure. The Fe II lines on the other hand, had good range in equivalent widths. We therefore relied upon Fe II lines to derive microturbulence. The microturbulence was derived by requiring that weak, medium and strong lines give a consistent value of abundance.

The final atmospheric parameters derived for the program stars are given in Table 2, along with their radial velocities relative to the Sun and to the Local Standard of Rest (LSR). The $\log(L/L_\odot)$ values in Table 2 were estimated from the effective temperatures determined spectroscopically, and the calibration of Schmidt-Kaler (1982). For HD 172481 a red spectrum obtained at McDonald Observatory in May, 2000, allowed us to measure the three

components of the OI feature near 7774 Å. The combined equivalent width $W(7774) = 1.3 \text{ \AA}$ and the calibration of Arellano Ferro, Giridhar & Goswami (1991) lead to $M_v = -5.6$ or $\log(L/L_\odot) = 4.1$, which is in good agreement with the value 4.5 obtained from Schmidt-Kaler's calibration. For homogeneity we have adopted the latter value for our discussion about the evolutionary status of this object in Sect. 6.

4. Uncertainties in the Elemental Abundances

The uncertainties in the derived abundances are caused by errors in the determination of the atmospheric parameters, in the equivalent width measurements, and also in the quality of oscillator strengths. For spectra with S/N ratios larger than 50 the errors in the equivalent widths are between 5 and 8%. The errors in gf values vary from element to element. For Fe I lines, experimental values of good accuracies (better than 10%) do exist, for other Fe-peak elements the range in errors could be within 10 to 25%. For heavier elements, particularly for s -process elements, the errors could be larger than 25%. For the stars HD 725, HD 158616, HD 172481, HD 173638, HD 218753 and HD 331319 we could measure a very large number of unblended lines, and the estimated errors in T_{eff} , $\log g$ and ξ_t are $\pm 200 \text{ K}$, ± 0.25 and $\pm 0.2 \text{ km s}^{-1}$, respectively. The sensitivity of the derived abundances to changes in the model atmospheric parameters are described in Table 4 of Gonzalez et al. (1997) for two RV Tau stars. We have used the same grid of atmospheric models and the same database for line oscillator strengths, hence the procedure will not be repeated here. For the Fe-peak elements we could measure a sufficiently large number of lines and the gf values used being of good quality, we expect these abundances to be accurate within 0.2 to 0.25 dex. For heavier elements, particularly the s -process elements, the uncertainty could be above 0.3 dex. Similarly for light elements like oxygen where few lines are available the uncertainty could be above 0.3 dex. For HD 172324 and HDE 341617, we will discuss the uncertainties in their respective sections.

5. Results

In what follows, we present derived elemental abundances for individual stars.

5.1. HD 725

This star is an IRAS source (00091+5659). It was classified as F5Ib-II by Griffin & Redman (1960) suggesting a temperature of $\sim 6900 \text{ K}$ if we follow the calibration of Schmidt-Kaler (1982).

Using the *wby* photometry of Perry (1969), Olsen (1983), Hauck & Mermilliod (1998), reddening free colours and our own unpublished calibrations for F-G supergiant

Table 2. Physical and dynamical parameters derived for program stars

Star	T_{eff} (K)	$\log g$	ξ_t (km s^{-1})	$V_r(\text{hel})$ (km s^{-1})	$V(\text{LSR})$ (km s^{-1})	σ_{V_r} (km s^{-1})	$\log (L/L_{\odot})$
HD 725	7000	1.0	4.65	-56.9	-48.8	0.8	4.2
HD 9167	7250	0.5	4.20	-45.7	-40.2	1.1	4.2
HD 158616	7300	1.5	4.6	+68.8	+78.6	2.1	4.5
				+63.7	+78.5	1.5	
HD 172324	11000	2.5	5.0	-126.1	-106.4	1.1	2.7
	11500	2.5	7.5	-117.3	-97.5	2.5	
HD 172481	7250	1.5	4.60	-73.1	-76.9	1.8	4.1,4.5
	7250	1.5	5.10	-84.4	-74.0	2.1	
HD 173638	7500	1.5	4.30	+11.6	+26.9	1.2	4.5
HD 218753	8000	2.0	3.35	+3.2	+13.9	1.0	1.6
HD 331319	7750	1.0	5.35	-2.5	+15.8	1.5	4.5
HDE 341617	23000	3.0	15.00	+67.9	+87.8	2.9	4.6

stars, we estimated $T_{\text{eff}} = 6900$ K. Balmer line fitting was not performed because the profiles display complex structure and underlying emission is suspected.

Table 3. Elemental Abundances for HD 725

Species	$\log \epsilon_{\odot}$	[X/H]	s.d.	N	[X/Fe]
C I	8.55	-0.38	± 0.03	3	-0.08
Na I	6.32	+0.21	± 0.08	3	+0.51
Mg I	7.58	-0.18	± 0.25	4	+0.12
Si I	7.55	+0.05	± 0.03	2	+0.35
Si II	7.55	+0.12		1	+0.42
S I	7.21	-0.10	± 0.17	3	+0.20
Ca I	6.35	-0.16	± 0.10	12	+0.14
Sc II	3.13	-0.03	± 0.23	7	+0.27
Ti II	4.98	-0.31	± 0.08	6	-0.02
Cr I	5.67	-0.16	± 0.17	7	+0.14
Cr II	5.67	-0.19	± 0.16	11	+0.11
Mn I	5.39	-0.27	± 0.12	6	+0.03
Fe I	7.51	-0.26	± 0.14	51	
Fe II	7.51	-0.33	± 0.15	11	
Ni I	6.25	+0.04	± 0.14	3	+0.33
Y II	2.23	+0.12	± 0.15	3	+0.42
Zr II	2.60	-0.07	± 0.13	2	+0.22
Ba II	2.13	+0.15		1	+0.45
Ce II	1.58	-0.17	± 0.13	2	+0.13

Notes – The solar abundances are taken from Grevesse, Noels & Sauval (1996).

– N is the number of lines included in the calculation.

The finally adopted parameters are $T_{\text{eff}} = 7000$ K, $\log g = 1.0$ and $\xi_t = 4.65 \text{ km s}^{-1}$. We relied upon Fe II lines for calculating microturbulence velocity. A large number

of Fe I lines were measured and used in estimating T_{eff} . Also neutral and ionized lines of Ti and Cr were employed to derive a satisfactory pair of T_{eff} and $\log g$ values. A competing solution could have been $T_{\text{eff}} = 7200$ K, $\log g = 1.5$ but the adopted parameters gave marginally better consistency in the abundances of neutral and ionized lines. HD 725 appears to be very marginally metal-poor (Table 3) and it has a moderately high radial velocity of -57 km s^{-1} . The elemental abundances relative to Fe, i.e. $[\text{X}/\text{Fe}] = [\text{X}/\text{H}] - [\text{Fe}/\text{H}]$ ¹, given in the last column of Table 3 and subsequent tables, were calculated adopting the average value of $[\text{Fe}/\text{H}]$ from Fe I and Fe II lines. For HD 725 the $[\text{X}/\text{Fe}]$ values are similar to those in normal unevolved stars for many elements. $[\text{Na}/\text{Fe}] = +0.5$ dex indicates relative enrichment of Na which is a well-known feature of A-F supergiants (Takeda & Takada-Hidai 1994, Venn 1995a, b). But Na I abundances are likely to be affected by non-LTE effect. Non-LTE analysis of Na I lines has been done by Gigas (1986), Takeda & Takada-Hidai (1994) and others. The errors introduced by the neglect of non-LTE becomes more severe for higher temperatures. According to Takeda & Takada-Hidai (1994), the $\Delta \log \epsilon$ in Na I lines at 5682, 5688, 6154 and 6160 Å is -0.09 , -0.10 , -0.07 and -0.07 dex respectively at temperature 7500 K. At temperature 7000 K the correction is 0.01 dex smaller for all lines than the values mentioned above. According to Gigas (1986) the non-LTE correction could be $+0.1$ to $+0.2$ dex. The use of $[\text{Na}/\text{Ca}]$ instead of $[\text{Na}/\text{Fe}]$ is recommended by Lambert (1992) for LTE calculations. The $[\text{Na}/\text{Ca}]$ of $+0.4$ dex found from our analysis shows that Na enrichment appears to be real. The Na might have been synthesized in the H-burning region where the NeNa cycle might operate together with the CNO cycle. The

¹ using the spectroscopic notation $[\text{X}/\text{H}] = \log [(X/H) - (X/H)_{\odot}]$

suggestion that the proton capture on ^{22}Ne could lead to enhancement of ^{23}Na is followed up by Langer, Hoffman & Sneden (1993). These authors used a nuclear reaction network to examine the changes in abundances caused by proton capture at $T_9 = 0.040$. Mixing of this region just below the oxygen shell over a timescale of 30,000 yr would cause enhancement of ^{14}N , ^{23}Na and ^{27}Al at the expense of ^{16}O , ^{22}Ne , ^{25}Mg and ^{26}Mg . These authors also suggested that the abundant ^{20}Ne could also be transformed into ^{23}Na on longer timescales, and pointed out that the depletion of ^{25}Mg and ^{26}Mg would not modify the Mg abundance. Globular cluster giants are known to display Na – O anticorrelation as reported by Sneden et al. (1991) and Kraft et al. (1992). Since our spectrum does not go to wavelengths longer than 6800 Å, we could not measure N I abundance nor could we measure the O abundance. In metal-poor stars, relative enrichment of α elements is to be expected but the effect becomes evident for $[\text{Fe}/\text{H}] < -0.5$ dex. At $[\text{Fe}/\text{H}] -0.2$ to -0.3 dex the spread in observed abundances is large and a large number of stars have $[\alpha/\text{Fe}] \sim 0$. For HD 725, the α element Si shows small enhancement but the number of lines used are woefully small to make a definite claim.

Among Fe-peak elements, Ni, represented by 3 Ni I lines, appears to be enriched, with $[\text{Ni}/\text{Fe}]$ of +0.3 dex. HD 218753 and HD 173638 of our sample show a positive $[\text{Ni}/\text{Fe}]$ but the value is not above abundance errors. As such, for HR 725 the value is slightly above twice the standard error, nevertheless a more extensive analysis based on a larger number of lines is required to see if the enrichment is real. Luck & Bond (1983, 1985) have reported $[\text{Ni}/\text{Fe}] \sim 0$ for metal-poor star. Wheeler, Sneden & Truran (1989) on the other hand report very large scatter in $[\text{Fe}/\text{H}]$ vs. $[\text{Ni}/\text{Fe}]$ relation. These authors suggest that non-zero $[\text{Ni}/\text{Fe}]$ can be observed at all metallicities.

Another interesting finding is $[\text{Y}/\text{Fe}]$ of +0.4 dex. The three Y II lines used are quite well separated and have good estimates of oscillator strengths, but out of the three lines, one is a little strong. The same is true for the Ba II line used. Mild enrichment of s -process elements in the moderately metal-poor star HD 70379 has already been reported (Reddy 1996). Hence, our average $[\text{s}/\text{Fe}]$ ratio +0.3 does not come as a surprise. In addition, its radial velocity of -57 km s^{-1} lends support to our view that it is a low-mass evolved object. These results are highly suggestive though not conclusive indicators of evolution beyond the red giant branch. However, making use of its proper motions and parallax from the Hipparchos catalogue we have calculated the galactocentric velocities $\Pi = -32.6 \text{ km s}^{-1}$, $\Theta = +190.3 \text{ km s}^{-1}$ and $Z = +5.4 \text{ km s}^{-1}$ that indicate a space velocity of 193.2 km s^{-1} with a small pitch angle of 9.7° relative to the circular orbit and on the galactic plane. This indicates that the star is at a lower galactic latitude than the Sun and placed in a mildly eccentric orbit.

5.2. HD 9167

This star has infrared flux and is an IRAS source (01285+6115). It appears to be another moderately metal-poor star (Table 4). We did not find any remarkable abundance peculiarity for this object. With radial velocity of -45 km s^{-1} and $[\text{Fe}/\text{H}]$ of -0.3 dex, one could be optimistic of seeing positive $[\alpha/\text{Fe}]$. Unfortunately, we could not measure good Si I and Si II lines and Mg, Ca and Ti do not show any enrichment. But on the other hand, for stars with $[\text{Fe}/\text{H}]$ in the range of 0.0 to -0.5 dex, the observed abundance ratios of α -process elements have very large scatter, hence finding evolutionary changes is almost as probable as not finding them. Likewise HD 725, rather large radial velocity implies a space velocity of 208.2 km s^{-1} with a small pitch angle of 5.7° relative to the circular orbit and on the galactic plane. The orbit is even less eccentric than that of HD 725 and it is at a lower galactic latitude than the Sun.

Table 4. Elemental Abundances for HD 9167

Species	$\log \epsilon_\odot$	$[\text{X}/\text{H}]$	s.d.	N	$[\text{X}/\text{Fe}]$
Mg I	7.58	-0.37	± 0.15	2	-0.04
Ca I	6.35	-0.22	± 0.09	6	+0.12
Sc II	3.13	-0.28	± 0.09	3	+0.05
Ti II	4.98	-0.48	± 0.17	10	-0.15
Cr I	5.67	-0.19		1	+0.15
Cr II	5.67	-0.27	± 0.21	9	+0.07
Mn I	5.39	-0.35		1	-0.02
Fe I	7.51	-0.32	± 0.16	29	
Fe II	7.51	-0.35	± 0.21	10	
Y II	2.23	-0.23	± 0.27	3	+0.11
Ba II	2.13	-0.22	± 0.09	2	+0.12

Notes – same as Table 3.

5.3. HD 158616

This star is an IRAS source (17279–1119) with significant infrared fluxes at shorter wavelengths.

The spectral type as listed in the SAO catalogue is F8, which suggests a temperature between 6100–6200 K (Schmidt-Kaler 1982), depending upon the luminosity class. No photometric data are available and hence no other temperature estimate was made. Two spectra were obtained for this star at the OHP. The S/N for these two spectra are 34 and 53. Since the spectrum from July 7 is better, it was decided to use it to determine T_{eff} , $\log g$ and ξ_t , complete the abundance analysis and then simply use the same parameters on the lower S/N spectrum from July 6 to verify the abundance pattern. The results are given in Table 5. The second entries for each species are

for the lower S/N spectrum. One can see that the results from both spectra are in a good agreement.

Table 5. Elemental Abundances for HD 158616

Species	$\log \epsilon_{\odot}$	[X/H]	s.d.	N	[X/Fe]
C I	8.55	-0.25	± 0.20	4	+0.33
		-0.23	± 0.14	4	+0.35
O I	8.87	-0.54	± 0.02	2	+0.04
		-0.55		1	+0.03
Na I	6.32	+0.05	± 0.01	3	+0.63
		-0.05		1	+0.49
Mg I	7.58	-0.40	± 0.11	3	+0.18
		-0.56		1	-0.02
Si I	7.55	+0.03	± 0.17	3	+0.61
Si II	7.55	-0.06	± 0.17	2	+0.52
		+0.04	± 0.47	2	+0.58
S I	7.21	+0.08	± 0.12	6	+0.66
		+0.10	± 0.01	2	+0.64
Ca I	6.35	-0.36	± 0.16	12	+0.22
		-0.34	± 0.31	9	+0.20
Sc II	3.13	+0.00	± 0.27	8	+0.58
		-0.09	± 0.24	4	+0.45
Ti I	4.98	+0.08	± 0.20	2	+0.66
		+0.18		1	+0.72
Ti II	4.98	-0.01	± 0.19	13	+0.57
		-0.13	± 0.11	8	+0.41
Cr I	5.67	-0.55		1	+0.03
Cr II	5.67	-0.39	± 0.14	14	+0.19
		-0.47	± 0.22	7	+0.07
Mn I	5.39	-0.17		1	+0.41
Fe I	7.51	-0.58	± 0.15	39	
		-0.61	± 0.18	20	
Fe II	7.51	-0.57	± 0.19	19	
		-0.51	± 0.19	7	
Ni I	6.25	-0.41	± 0.08	4	+0.17
		-0.39		1	+0.19
Zn I	4.60	-0.48	± 0.02	2	+0.10
		-0.40		1	+0.18
Y II	2.23	+0.37	± 0.25	4	+0.95
		+0.48	± 0.03	2	+1.02
Ba II	2.13	+0.04	± 0.22	3	+0.62
		+0.10	± 0.20	2	+0.64
La II	1.21	-0.11		1	+0.47
Ce II	1.58	+0.13	± 0.22	5	+0.71
		+0.21		1	+0.75

Notes – same as Table 3.

– second entries are results from a lower S/N spectrum

HD 158616 was also studied by Van Winckel (1995; 1997). While he had better data for C,N,O due to extended coverage in the long wavelength region, for other elements, our spectra contained more lines per element, and more elements are included. This star is Fe-poor by a factor of 4 or so and shows very clear indications of CNO process-

ing and enrichment of s -process elements. We get $C/O \sim 1$ whereas Van Winckel (1995) got this ratio significantly larger than one (see Table 14). His carbon abundance is based on more lines in the 7100 Å region. His choice of T_{eff} is also hotter than our adopted value that can also account for the higher carbon abundance derived. Van Winckel (1995) found $[N/Fe]$ of +0.2 dex. This clearly shows that the star has gone through CNO cycle and its products have been brought to the surface. The carbon enrichment could be caused by the helium-shell burning when oxygen is also manufactured. The enhancement of Si and S could be present in ISM from which the star is formed. With the $[Fe/H]$ of -0.6 dex, the star is moderately metal-poor and therefore it is possible that the parent ISM might have received ejecta from type II SNe. Although the effect of departure from LTE has been discussed for the light elements C,N,O and also for Mg by different investigators, we did not come across similar discussion on Si and S. Hence, at this stage, we chose not to offer any detailed explanation. The most interesting feature of the derived abundances is definitely the enrichment of s -process elements Y, Ba, La and Ce. This star is undoubtedly a post-AGB star that has brought the products of helium burning as well as elements formed by s -processing to the surface. Our analysis covers the light s -process element Y (one of the three elements referred as ls) and the heavy s -process elements Ba, La and Ce, representing heavy (hs) s -process elements. We have made an estimate of $[hs/ls]$. We have not corrected the ls-index for the lack of light elements Sr and Zr since for light elements the odd-even effect is not strong as pointed out by Van Winckel & Reyniers (2000). We estimated $[hs/ls] = -0.3$ and $[ls/Fe]$ of +1.0. When plotted on the $[hs/ls]$ vs. $[ls/Fe]$ plot of Busso et al. (1999), (their Fig. 7 giving theoretical predictions), we found $\tau_0 \sim 0.22 \text{ mbarn}^{-1}$. Incidentally, the data point falls near the thick line which for solar metallicity would indicate $C/O = 1$ but for $[Fe/H]$ of -0.6, it indicates a $C/O \sim 3$, whereas we get $C/O \sim 1$. This reduction of carbon abundance, while hs and ls indices point to larger C/O added to small but significant enhancement of nitrogen, as reported by Van Winckel (1995), strongly favour the hot bottom burning scenario described and discussed in section 5.5. More extensive coverage of s -process elements will enable a meaningful comparison with third dredge-up models developed by Straniero et al. (1995) and Busso et al. (1995).

Another star of similar temperature and showing a similar trend in abundances is HR 6144 (Luck et al. 1990), however, in this star, the s -process enhancement is not so significant and C/O is less than 1.

5.4. HD 172324

This star has been classified as B9Ib by Morgan & Roman (1950) which suggests a temperature of 10280 K (Schmidt-Kaler 1982). The Strömgen colours (Hauck & Mermil-

liod 1998) however point towards higher temperature: 13100 K using the calibration of Napiwotzki, Schönberner & Wenske (1993). An independent temperature calibration of the Geneva photometric system (Cramer & Maeder 1979) gives a temperature of 13215 K.

The He I lines have been used to estimate T_{eff} and luminosity class of the star. Didelon (1982) gives very useful plots of the dependence of many He I, Si II, Mg II, C II, O II and N II line strengths on the spectral type and luminosity class. The equivalent widths in our spectrum for the He I lines at 4120, 4143, 4387 and 4471 Å very clearly suggest a spectral type of B9. A luminosity class Ib was suggested by the strengths of Si II line at 4128 Å, Mg II line at 4481 Å and C II feature at 4267 Å, this is in good agreement with the spectral type above.

An estimate of T_{eff} has been made by requiring the He I lines to give solar abundance. The best estimate is 11500 K. Given the class Ib, $\log g$ must not be very different from 2.0. In any case, at the high temperature end the Kurucz (1993) models do not reach very low gravities. Fortunately, Mg I and Mg II lines are present in the OHP spectrum and Si II and Si III lines can be measured on the McDonald spectrum. Our derived T_{eff} and $\log g$ appear to be good estimates for the epoch of OHP spectrum. However there is indication that at the epoch at which the McDonald spectrum was taken, the gravity was somewhat lower.

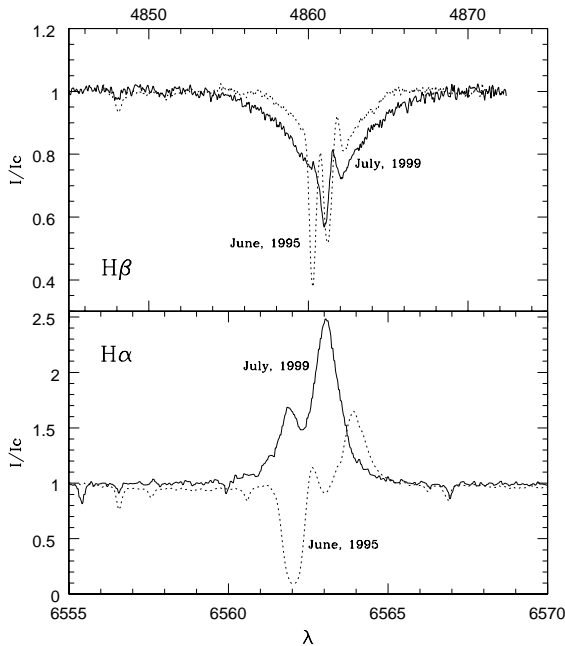


Fig. 1. H_{α} and H_{β} variations exhibited by HD172324 in two spectra taken 4 years apart: June 1995 at McDonald and July 1999 at OHP.

This star appears to be deficient in Fe by a factor of 3-4 and has a large radial velocity of -110 km s^{-1} mak-

Table 6. Elemental Abundances for HD 172324

Species	$\log \epsilon_{\odot}$	[X/H]	s.d.	N	[X/Fe]
He I	10.99	-0.08	± 0.35	4	+0.54
He I*	10.99	-0.19	± 0.35	12	+0.44
C II*	8.55	-1.30		syn	-0.68
O I	8.87	+0.41	± 0.20	2	+1.03
O I*	8.87	+0.26	± 0.19	4	+0.89
Ne I*	8.09	+0.05		1	+0.68
Mg I*	7.58	-0.63		1	0.00
Mg II	7.58	-0.66	± 0.17	2	-0.04
Mg II*	7.58	-0.65	± 0.12	3	-0.02
Al I	6.47	-0.59		1	+0.03
Al II*	6.47	-0.65		1	-0.02
Si II	7.55	-0.16	± 0.03	2	+0.47
Si II*	7.55	-0.29	± 0.14	6	+0.39
Si III	7.55	+0.25		1	+0.88
S II	7.21	-0.19		1	+0.43
S II*	7.21	-0.47		1	+0.16
Ti II	4.98	-0.03	± 0.24	8	+0.59
Ti II*	4.98	-0.28	± 0.33	3	+0.35
Cr II	5.67	-0.43	± 0.19	11	+0.19
Cr II*	5.67	-0.48	± 0.28	3	+0.15
Fe II	7.51	-0.62	± 0.17	17	
Fe II*	7.51	-0.63	± 0.11	11	

Notes – same as Table 3.

$-T_{\text{eff}} = 11000 \text{ K}$, $\log g = 2.5$ and $\xi_t = 7.00 \text{ km s}^{-1}$ for McD spectrum

$-T_{\text{eff}} = 11500 \text{ K}$, $\log g = 2.5$ and $\xi_t = 5.40 \text{ km s}^{-1}$ for OHP spectrum

* result from OHP spectrum.

ing it a likely halo or old disk object. Carbon abundance is very important in ascertaining the evolutionary status. We could observe only the blend at 4267 Å while supposedly strong lines at 6578 and 6582 Å were too weak to be measured. By computing the blend of two C II lines at 4267 Å we find [C/H] of -1.3 dex, for which Takeda, Takada-Hidai & Kotake (1996) found zero non-LTE correction. In the neighbourhood of $T_{\text{eff}} 10000 \text{ K}$ the non-LTE abundance correction for carbon using C I lines is ~ -0.4 dex (Venn 1995b). Our iron abundance is based on Fe II lines that are not strongly affected by non-LTE effects. For O I line at 6156-6158 Å the non-LTE correction is ~ -0.3 dex (Takeda & Takada-Hidai 1998).

For A-type supergiants of solar metallicity, Venn (1995a) found a mean enrichment of ~ 0.6 dex for Na and ~ 0.3 dex for S. Venn (1995b) reported CNO abundances for the same sample after applying non-LTE corrections to the derived abundances. The mean values found were: [C/H] = -0.4 dex, [N/H] = $+0.08$ dex and [O/H] = -0.2 dex. Nevertheless, the hottest star of Venn's sample, HD 161695, is about 1500 K cooler than HD 172324.

McErlean, Lennon & Dufton (1999) have plotted LTE and non-LTE line profiles for a range of temperatures 10000 K to 35000 K. At 11000 K the non-LTE correction for C II lines at 4267 Å is very small, in agreement with the prediction of Takeda, Takada-Hidai & Kotake (1996). Hence our values $[C/H] = -1.3$ dex and $[C/Fe] = -0.68$ dex are realistic estimates.

For an A-type star of solar metallicity, a mean value $[C/H] = -0.4$ was reported by Venn (1995b), whereas for B supergiants McErlean, Lennon & Dufton (1999) report mean values of $[C/H] = -0.35$ dex and $[O/H] = -0.32$. After applying non-LTE correction for oxygen we get $[O/H]$ of +0.1 dex and $[O/Fe]$ of +0.7 dex. Our derived carbon and oxygen abundances in Table 6 are much different from what is expected for a young B9 supergiant. It has been suggested by Boothroyd & Sackmann (1999) that the carbon deficiency can also be caused by deep circulating mixing below the base of the convective envelope followed by cool bottom processing (CBP) of the CNO isotopes. They also showed that the CBP became more extensive at reduced metallicities or at low masses. The high radial velocity for HD 172324 (more than 100 km s^{-1}) and significantly low $[Fe/H]$ makes it very likely that it has experienced CBP.

The only trace of an odd Z element we could observe was a single line of Al I, providing $[Al/Fe] \sim 0$. One does not see $[Al/Fe] \sim +0.30$ dex reported by Edvardsson et al. (1993), but with single line being used in our study not much significance could be attached to our estimated $[Al/Fe]$.

Hot stars at high galactic latitude were studied by Conlon et al. (1993a) who found very large Fe and C deficiencies in them. But the stars studied by these authors are much hotter than HD 172324. Nevertheless, the abundance pattern of HD 172324 is similar to those studied by Conlon et al. (1993a;b) and McCausland et al. (1992). This star being most likely an oxygen-rich post-AGB star deserves an extended analysis covering CNO and as significant spectral variations can be seen in four years (see Fig. 1), a monitoring of hydrogen line profiles over long time scales will be of interest.

5.5. HD 172481

This star shows light variations of very small amplitude, ± 0.15 mag (Van Winckel 1995). The spectral energy distribution of this star has an unusual multi-peaked shape (Bogart 1994). It was included in the study of Van Winckel (1995) who, by fitting the observed flux distribution to that of Kurucz (1993) model atmosphere, derived $T_{\text{eff}} = 7000$ K. Van Winckel also found that the strength of emission components in hydrogen lines varied strongly. From the study of radial velocity variation spread over a decade, he reported that there is not enough evidence for the binarity of the star. However, his spectra show considerable line splitting attributed to the passage of a shock. Fortu-

nately, we obtained the spectrum of HD 172481 when the atmosphere of the star was stable and therefore no line splitting was observed, as can be seen in the Fig. 2.

Table 7. Elemental Abundances for HD 172481

Species	$\log \epsilon_{\odot}$	$[X/H]$	s.d.	N	$[X/Fe]$
Li I	1.16	+2.54 :		1	+3.16 :
C I	8.55	-0.62	± 0.21	12	-0.01
N I	7.97	-0.63	± 0.10	3	-0.02
O I	8.87	-0.58	± 0.05	2	+0.04
Mg I	7.58	-0.13	± 0.21	2	+0.48
Mg II	7.58	-0.06	± 0.54	3	+0.55
Si I	7.55	-0.05	± 0.17	6	+0.57
Si II	7.55	-0.10	± 0.06	3	+0.52
S I	7.21	-0.04	± 0.16	7	+0.58
K I	5.12	-0.28		1	+0.34
Ca I	6.35	-0.28	± 0.19	12	+0.34
Sc II	3.13	-0.20	± 0.23	6	+0.41
Ti I	4.98	-0.31		1	+0.31
Ti II	4.98	-0.28	± 0.30	6	+0.34
V II	4.00	-0.00	± 0.14	2	+0.62
Cr I	5.67	-0.34	± 0.05	3	+0.28
Cr II	5.67	-0.41	± 0.16	10	+0.21
Mn I	5.39	-0.51	± 0.11	3	+0.11
Fe I	7.51	-0.62	± 0.15	43	
Fe II	7.51	-0.61	± 0.14	13	
Ni I	6.25	-0.31	± 0.22	6	+0.30
Zn I	4.60	-0.23	± 0.08	2	+0.39
Y II	2.23	+0.08	± 0.26	4	+0.69
Zr II	2.60	-0.14		1	+0.46
Ba II	2.13	+0.03	± 0.20	2	+0.65
La II	1.21	-0.55	± 0.14	2	+0.07
Ce II	1.55	-0.24	± 0.19	7	+0.38
Nd II	1.50	+0.03	± 0.09	3	+0.64
Eu II	0.51	+0.24		1	+0.86

Note – same as Table 3.

Sadly, the S/N ratio of our spectrum is not very high. We could measure very few lines of important elements like C and O, hence we were not satisfied with the limited data to carry out abundance analysis. But it was known beyond doubt that the star is highly evolved since we could identify lines of C I and also saw Li I line at 6708 Å. However, the Li I feature was falling at the end of our CCD frame and was showing distinct doubling. One component coming nearest to Li I wavelength gave $\log \epsilon(\text{Li})$ of 1.8. But S/N being very poor at the end of the CCD frame, we decided to follow this object with more spectra. At our request, David Yong of McDonald Observatory got a spectrum using the 2dcoude echelle spectrograph at the 2.7m telescope of McDonald Observatory on May 13, 2000. The spectrum has resolution of 30,000 and wide spectral coverage from 3900 Å to 10200 Å. In this spectrum, we

found Li I feature to be single with some asymmetry in the blue wing but much deeper than in July 1999. In all HD 172481 spectra, the H_γ has a broad absorption, a narrow absorption and a possible red shifted emission component. The H_β also has a broad absorption and a narrow absorption at the centre of broad absorption. There is no indication of emission component. The H_α has a complex profile with one shallow absorption, one deep absorption that has emission components in both the wings. The blue emission component is stronger than the red one.

The extensive spectral coverage of McDonald spectrum enabled us to measure a large number of unblended lines for several light and heavy elements. As one can see from the Table 7, we could carry out a very comprehensive analysis of this object.

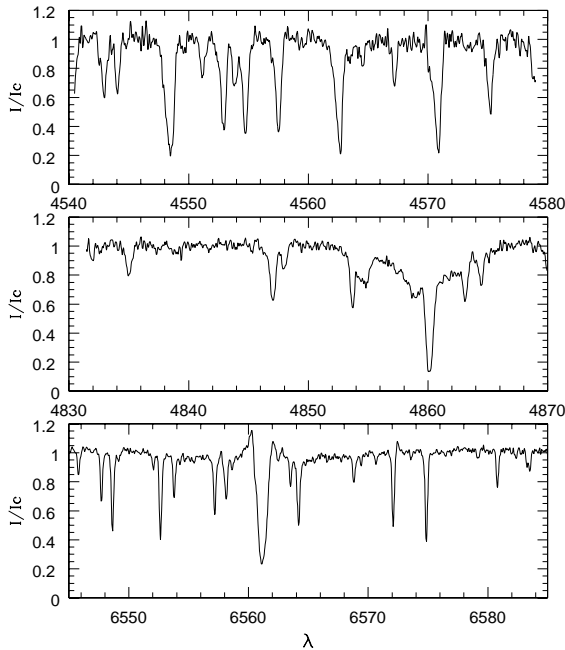


Fig. 2. Three spectral regions in the spectrum of HD 172481 clearly showing no line splitting. Hence we believe the star was in a stable phase.

From Fe I and Fe II lines we derived $T_{\text{eff}} = 7250$ K and $\log g = 1.5$ and was supported by Si I, Si II, Mg I and Mg II lines. We derived the Li abundance by spectrum synthesis. All the four components of Li I feature at the 6708 Å region were included. We find $\log \epsilon(\text{Li})$ of +3.7, which is surprisingly high. We were puzzled by the change in appearance of Li I feature at 6707, so on August 11 one more spectrum was obtained with the same set-up and by the same observer. The spectrum again showed a suggestion of doubling at the line core though the components were not well separated. It is not clear if the line is splitting periodically or the emission at the core is causing it to appear double. The overall strength of Li I feature

in the August spectrum has reduced. For May 2000 spectrum, our estimated Li abundance (derived by synthesis) is shown in Table 7 with a colon. In the light of the large variation exhibited by Li I feature in strength as well as in profile shape, this value should be regarded with caution. However, the presence of Li I feature in the spectrum cannot be refuted. Another Li I feature at 6103 Å fell in between the echelle orders and therefore could not be used.

We could measure a large number of C I lines to estimate the carbon abundance. The three N I lines in the near infrared also enabled us to derive the nitrogen abundance. We get $[\text{N}/\text{Fe}] \sim 0$ for HD 172481 whereas for HD 158616 $[\text{N}/\text{Fe}] = +0.3$ is reported by Van Winckel (1995). The estimated C/O is +0.43. The element Li is considered a fragile element that gets destroyed in the course of evolution. The primordial abundance of Li (based on population II objects) is considered near $\log \epsilon(\text{Li}) = 2.2$. The excess abundance must therefore be caused by AGB evolution of HD 172481 or might owe its origin to binarity.

Our analysis covers light *s*-process elements (ls) Y and Zr and heavy *s*-process elements (hs) Ba, La, Ce and Nd. We derive a mean $[\text{ls}/\text{Fe}]$ of 0.6 and mean $[\text{hs}/\text{Fe}]$ of 0.4. That leads to $[\text{hs}/\text{ls}]$ of -0.2 . With this value of $[\text{hs}/\text{ls}]$ and $[\text{Fe}/\text{H}]$ of -0.6 this star is remarkably similar to IRAS 04296+3429 and IRAS 19500-1709 studied by Van Winckel & Reyniers (2000), although $[\text{ls}/\text{Fe}]$ and $[\text{hs}/\text{Fe}]$ are much larger for these two stars.

The stars mentioned above and HD 158616 are very interesting post-AGB objects as they are, most likely, evolved from intermediate-mass stars (IMS). According to Travaglio et al. (1999), stars in the mass range 4 - 8 M_\odot , activate $^{22}\text{Ne}(\alpha, n)^{25}\text{Mg}$ reaction during their TP-AGB phase more effectively than the low-mass stars due to the high temperatures reached at the bottom of the convective pulse ($T_{\text{max}} \leq 3.5 \times 10^8$ K). IMS contribute more to the first *s*-peak represented by the elements Sr, Y and Zr. Actually, the number of known post-AGB IMS is very small. For IMS, the formation of a ^{13}C pocket is less certain because of the reduced mass of the H-He intershell by about one order of magnitude. It is shown by Straniero et al. (1997) and Gallino et al. (1998) that the ^{13}C neutron source active during the interpulse phase of low-mass TP-AGB accounts for most of the production of the second *s*-peak elements Ba, La, Ce, Sm and Eu.

It is obvious from the relative enhancement of Y and Sr presented in Tables 5 and 7 that HD 158616 and HD 172481 belong to the relatively rare post-AGB IMS. We would therefore try to understand the observed abundances of HD 172481 in the framework of AGB models developed by Lattanzio and others for IMS.

Lattanzio (1997) in his AGB calculation has predicted that for stars more massive than $4M_\odot$ the bottom of the convective envelope penetrates into the hotter regions of the envelope where proton captures already modified the original CNO composition. This is called "hot bottom burning" (HBB) and results in many important changes

in chemical composition of the envelope. Lattanzio (1997) predicted the production of Li by the Cameron-Fowler mechanism operating at bottom of the envelope. Sackmann & Boothroyd (1992) showed that $\log \epsilon(\text{Li}) \sim 4.5$ could be produced in stars with bolometric magnitude between -6 and -7 when the temperature at the base of the convective envelope exceeds 50×10^6 K. From the study of AGB stars in SMC and LMC, Smith, Plez & Lambert (1995) found them to have bolometric magnitudes in the range -6 to -7.2 and to show lithium values of $\log \epsilon(\text{Li}) \sim 1.0 - 4.0$. However, these are cool luminous S stars.

Lattanzio (1997) also predicted the destruction of carbon via CN cycle that could prevent C/O ratio from exceeding one. Theoretical models for AGB stars of mass 4, 5 and 6 M_{\odot} computed by Boothroyd, Sackmann & Ahern (1993) encountered HBB with a temperature at the base of the convective envelope reaching 80×10^6 K. These models predict C/O of 0.4 to 0.5 for $\sim 10^3$ yr on the AGB.

Table 8. Elemental Abundances for HD 173638

Species	$\log \epsilon_{\odot}$	[X/H]	s.d.	N	[X/Fe]
C I	8.55	-0.16	± 0.13	5	-0.09
Mg I	7.58	-0.05	± 0.12	5	+0.03
Si I	7.55	+0.36	± 0.12	2	+0.44
Si II	7.55	+0.41		1	+0.49
Ca I	6.35	+0.04	± 0.25	12	+0.12
Ca II	6.35	-0.03		1	+0.05
Sc II	3.13	+0.16	± 0.18	6	+0.24
Ti I	4.98	+0.01		1	+0.09
Ti II	4.98	-0.1	± 0.18	17	-0.04
Cr I	5.67	+0.08	± 0.07	3	+0.16
Cr II	5.67	-0.02	± 0.18	15	+0.06
Mn I	5.39	+0.00		1	-0.08
Fe I	7.51	-0.07	± 0.13	62	
Fe II	7.51	-0.08	± 0.14	19	
Ni I	6.25	+0.06	± 0.17	7	+0.14
Zn I	4.60	-0.06	± 0.05	2	+0.02
Y II	2.23	+0.02	± 0.22	5	+0.10
Zr II	2.60	-0.02		1	+0.06
Ba II	2.13	+0.15	± 0.04	2	+0.23
Ce II	1.58	+0.02		1	+0.10
Nd II	1.48	+0.11		1	+0.19

Note – same as Table 3.

The abundance pattern of HD 172481 bears some resemblance to those found for HR 7671 though the latter is more metal-poor. Interestingly, HR 7671 also shows the Li I feature though Li is not as overabundant as in HD 172481. The estimated C/O for HR 7671 is 0.4. The mean $[\alpha/\text{Fe}]$ is lesser than what we find for HD 172481 but $[\text{s}/\text{Fe}]$ is comparable.

The existence of objects like HD 172481 and HR 7671 lend further support to the HBB scenario, put forward to explain the paucity of carbon-rich stars among AGB stars. The observed variation of Li I feature in HD 172481 makes it a very promising candidate for binarity search.

While the present paper was under the refereeing process, the referee called our attention to the then unpublished work on HD 172481 by Reyniers & Van Winckel (2001). Thus a comparison with their results is most appropriate. These authors have derived atmospheric parameters ($T_{\text{eff}} = 7250$ K and $\log g = 1.5$) that are in excellent agreement with those derived by us. A small difference in ξ_t of 0.6 km s^{-1} is seen. These authors also find a large lithium abundance similar to our finding. The $[\text{Fe}/\text{H}]$ and other Fe-peak elements have very good agreement. The *s*-process elements La, Nd and Eu however, show some disagreement. We have measured 3 lines of Nd II so we are surprised by the lower limits placed by these authors. For Eu, we measured a fairly clean line at 6645 \AA whereas Reyniers & Van Winckel used spectrum synthesis. It should be noted that the oscillator strengths used by these authors are quite different from those employed by us, that can possibly explain the abundance differences for the *s*-process elements. The *gf* values for the lines of these elements are known to have larger uncertainties compared to those of the Fe-peak elements. Another important finding by Reyniers & Van Winckel is the detection of a red luminous companion, found from the presence of TiO bands in the red and also from the observed spectral energy distribution. As mentioned above, the presence of the companion might explain the Li I feature variations observed by us.

5.6. HD 173638

This star (HR 7055) was observed in the 13-Colour photometric system and its temperature was calculated by various approaches by Bravo Alfaro, Arellano Ferro & Schuster (1997). The photometric temperature estimates range between 7486 K and 8100 K. The spectrum being of $S/N = 95$, we could measure a large number of lines covering many important elements like C, α -process elements and Fe-peak elements. From the ionisation equilibrium of Fe I/Fe II, Cr I/Cr II, Ti I/Ti II, Si I/Si II and even Ca I/Ca II the atmospheric parameters are well-determined and listed in Table 2.

The star appears to have near-solar abundances for most elements except Si which is overabundant by a factor of 3 (Table 8). With its small radial velocity ($+11 \text{ km s}^{-1}$), it is most likely a young star belonging to the disk population. But it can serve as excellent calibrator of photometric indices in the 7500 K temperature range.

5.7. HD 218753

This star was classified as A5III by Cowley et al. (1969). These and the Sp.T. - Colour - T_{eff} calibration of Schmidt-Kaler (1982) give a temperature of 8091 K.

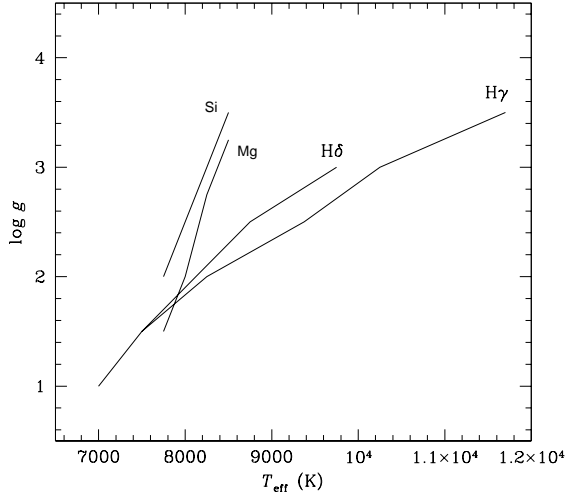


Fig. 3. H_γ , H_δ , Mg and Si loci for HD 218753.

Table 9. Elemental Abundances for HD 218753

Species	$\log \epsilon_\odot$	[X/H]	s.d.	N	[X/Fe]
C I	8.55	-0.49	± 0.18	5	-0.30
O I	8.87	-0.14		1	+0.05
Na I	6.32	+0.32	± 0.07	2	+0.51
Mg I	7.58	-0.27	± 0.16	5	-0.08
Mg II	7.58	-0.29	± 0.15	4	-0.10
Si I	7.55	+0.11	± 0.15	3	+0.20
Si II	7.55	+0.00	± 0.22	4	+0.26
S I	7.21	+0.17	± 0.09	2	+0.36
Ca I	6.35	-0.08	± 0.15	15	+0.11
Ca II	6.35	-0.09		1	+0.10
Sc II	3.13	+0.00	± 0.27	8	-0.19
Ti I	4.98	-0.27		1	-0.08
Ti II	4.98	-0.25	± 0.17	19	-0.06
Cr I	5.67	-0.01	± 0.38	3	+0.18
Cr II	5.67	-0.16	± 0.13	14	+0.03
Mn I	5.39	-0.23	± 0.06	3	-0.04
Fe I	7.51	-0.20	± 0.16	82	
Fe II	7.51	-0.18	± 0.13	30	
Ni I	6.25	-0.06	± 0.15	9	+0.13
Zn I	4.60	+0.18		1	+0.37
Y II	2.23	-0.24	± 0.21	7	-0.05
Zr II	2.60	+0.18		1	+0.37
Ba II	2.13	-0.08	± 0.16	2	+0.11

Notes – same as Table 3.

Photometric data in the Strömgen's system can also be used to estimate T_{eff} , through the $\beta - (b - y)$ relation of Crawford (1979) (his Table 1) and adopting $(b - y) = 0.236$ and $\beta = 2.773$ (Hauck & Mermilliod 1998). This leads to $(b - y)_o = 0.176$ and $E(b - y) = 0.054$. While $(b - y)_o$ leads to $(B - V)_o = 0.20 - 0.25$ (Crawford 1970), this implies $T_{\text{eff}} = 7800$ K.

Also, if the above colour excess and photometry are used in combination of Napiwotzki, Schönberner & Wenske's (1993) calibration we find $T_{\text{eff}} = 7200$ K. However, it must be emphasized that the calibration has been computed using only stars of luminosity classes V and IV, while HD 218753 could be of luminosity class III or II.

Balmer line fitting can also be used to estimate T_{eff} . Theoretical profiles have been extracted from Kurucz's (1993) models for H_α , H_β , H_γ and H_δ . The observed profiles were fitted with theoretical profiles of given T_{eff} and $\log g$. The solution is not unique but in fact the best fits define a locus on the $T_{\text{eff}} - \log g$ plane for each Balmer line. As underlying core emission may be present in some stars, we chose to fit the wings H_γ and H_δ . Following the above fitting process we found the loci for H_γ and H_δ profiles shown in Fig. 3.

In hot stars, magnesium and silicon lines can be used as T_{eff} indicators (since Fe I lines are strongly affected by non-LTE effects). Given a pair $(T_{\text{eff}}, \log g)$ one searches for abundance consistency between neutral and ionized lines of Mg and Si. Again, the solution is not unique but rather a locus on the $T_{\text{eff}} - \log g$ plane is defined for each element, as illustrated in Fig. 3. The intersections of the Mg and Si loci with the H_γ and H_δ loci point to the proper temperature and gravity. In this fashion we estimated T_{eff} between 7600 and 7900 K and $\log g$ between 1.75 and 2.0.

The turbulent velocity, ξ_t , was estimated from Fe II lines by requiring abundance to be independent of line strength. We found $\xi_t = 3.3 \text{ km s}^{-1}$.

For HD 218753 we finally adopted $T_{\text{eff}} = 8000$ K, $\log g = 2.0$ dex and $\xi_t = 3.3 \text{ km s}^{-1}$. With these parameters the abundances for the rest of the detected species were calculated and the results are given in Table 9.

For this star our spectrum has $S/N = 67$ and we could measure a large number of clean weak lines for most important elements. HD 218753 shows a significant carbon deficiency most likely caused by CNO processing. There is also a significant enrichment of sodium that has been found in many A-F supergiants as discussed before for HD 725 (Takeda and Takada-Hidai 1994). Among α -capture elements, only S shows enrichment above detection limit. These are indications of the star having experienced the first dredge-up (e.g. $[C/Fe] = -0.3$ dex). However its position in the H-R diagram of Fig. 5 is consistent with a $M \sim 1.5 - 2M_\odot$ and an age of about 7.9×10^8 yr.

Table 10. Elemental Abundances for HD 331319

Species	$\log \epsilon_{\odot}$	[X/H]	s.d.	N	[X/Fe]
C I	8.55	-0.33	± 0.30	5	-0.09
O I	8.87	+0.06	± 0.02	2	+0.30
Na I	6.32	-0.03		1	+0.21
Mg I	7.58	-0.32	± 0.21	3	-0.08
Mg II	7.58	-0.18	± 0.12	3	+0.06
Al I	6.47	+0.07		1	+0.31
Si II	7.55	-0.18	± 0.20	2	+0.06
S I	7.21	+0.29	± 0.18	5	+0.53
Ca I	6.35	-0.29	± 0.18	10	-0.05
Sc II	3.13	-0.19	± 0.22	5	+0.05
Ti II	4.98	-0.33	± 0.22	22	-0.09
V II	4.01	+0.19	± 0.16	3	+0.43
Cr I	5.67	-0.01	± 0.29	3	+0.23
Cr II	5.67	+0.02	± 0.14	18	+0.22
Mn I	5.39	-0.17		1	+0.07
Fe I	7.51	-0.27	± 0.16	48	
Fe II	7.51	-0.20	± 0.15	21	
Ni I	6.25	+0.00	± 0.22	4	-0.24
Ni II	6.25	-0.13		1	+0.11
Sr II	2.90	+0.01		1	+0.25
Y II	2.23	-0.58	± 0.09	3	-0.34
Ba II	2.13	-0.51	± 0.16	3	-0.27

Notes – same as Table 3.

5.8. HD 331319

This star is an IRAS source (19475+3119). The IR fluxes are quite large (Table 1), the heliocentric radial velocity is very small (-2.5 km s^{-1}). With a spectrum of $S/N = 98$ we could measure a large number of lines and hence derive the atmospheric parameters as well as abundances with good accuracy (Table 10). The star is Fe-poor by about 1.8 times, but shows significant enrichment of sulphur. The derived abundances are based on 5 good lines hence the derived sulphur abundance cannot be ascribed to measurement errors. Similarly, vanadium also shows some enrichment. Sulphur enrichment appears to be a common feature of our sample stars. The derived abundance of carbon for HD 331319 clearly indicates the effect of CN processing. The star is most likely a young massive disk supergiant or bright giant ascending the red giant branch. The IR fluxes are probably caused by material ejected at this evolutionary stage.

5.9. The proto-Planetary Nebula HDE 341617

It is an interesting object that has been showing relatively fast changes in temperature and brightness. It has faded from $m_v = 8.8$ reported in BD catalogue to $m_v = 11.4$ estimated by Stephenson (1986). Extensive photometry was taken up by Arkhipova et al. (1999), who found rapid light variations with an amplitude of up to

0.3 mag during 1996-1997. These authors also obtained a spectrum and describe the absorption and emission lines present. The light variations of HDE 341617 and spectral appearance confirmed the suggestion of Volk & Kwok (1989), based on IRAS color indices, that it is a candidate post-AGB star. From spectral type A5 given in HDE, it had changed to class Be (1986) as reported by Downes & Keyes (1988). A very extensive spectral investigation by Parthasarathy et al. (2000) has shown the star to have $T_{\text{eff}} = 22000 \text{ K}$ with large deficiency of carbon. These authors derived T_e of 10000 K and N_e of $2.5 \times 10^4 \text{ cm}^{-3}$ for the nebula from the study of emission lines. The spectra used by Parthasarathy et al. were taken in 1993. As this object presents rapid variations, we felt we could examine the spectrum at our epoch (1999) and study the changes. A comparison of the emission features common to Parthasarathy et al. (2000) 1993 spectrum and ours from 1999 is presented in Fig. 4. Fig. 4a shows that in 1999 the emission lines were weaker while Fig. 4b shows that the differences in equivalent widths are not a function of wavelength. Unfortunately, we did not observe any flux standard and so were unable to measure the fluxes in the emission lines. The shape of the pseudo continuum used for each echelle order may also be affected by instrumental sensitivity function. The large scatter is due to this fact. Weakening of lines (if it is not caused by resolution difference) might indicate further increase in temperature of the central star. Systematic monitoring of this fast evolving object could be very rewarding.

According to Arkhipova et al. (1999) HDE 341617 has a mass of $0.7 M_{\odot}$ with an envelope of $\sim 10^{-3} M_{\odot}$ undergoing rapid evolution towards the PN phase which, according to the predictions from Blöcker's (1995) models, should be reached within 100 years. This and the rapid photometric variations reported by Arkhipova et al. (1999), most likely caused by variations in the stellar wind, make the star a very interesting target for continuous monitoring.

We have two relatively low S/N spectra that were used for identification and measurement of absorption and emission lines. We present in Tables 11 and 12 the line strengths and velocities for absorption and emission lines for this object.

Several absorption lines of He I, O II, Si III and Fe II are detected. The radial velocity, for each individual line unambiguously identified is given in Table 11. For He I two groups of lines are identified at average velocities of $52.6 \pm 8.3 \text{ km s}^{-1}$ (4 lines) and $75.0 \pm 3.7 \text{ km s}^{-1}$ (4 lines). This suggests some stratification in the atmosphere. The rest of the species however average $73.3 \pm 2.9 \text{ km s}^{-1}$ (15 lines). The low dispersion in the radial velocity suggests that all these lines are formed in the same region of the stellar atmosphere and no stratification is evident.

The emission spectrum, formed in the outer envelope and/or in the nebulosity, consists of lines of Fe II, [Fe II], Fe III, [S II], O I, [N II] and Si II. The radial velocities of emission lines are all very consistent and average

$54.3 \pm 3.4 \text{ km s}^{-1}$. The difference of radial velocities between the absorption and emission lines indicates that the nebulosity expands at about 19 km s^{-1} . The Balmer lines show emission on top of the stellar absorption. The emission is shifted relative to the absorption and is consistent with the radial velocities of other emission features, showing that it is also produced in the same region.

Though the number of absorption lines were relatively small, we have done an abundance analysis for a few elements. The O II lines were used for fixing the microturbulence velocity. Since the line data was not adequate to do a detailed excitation equilibrium, we chose to use the temperature and gravity estimated by Parthasarathy et al. (2000) as starting value and tried models both hotter and cooler than their estimate. We got more consistent values for $T_{\text{eff}} = 23000 \text{ K}$, $\log g = 3.0 \text{ dex}$ and $\xi_t = 15.0 \text{ km s}^{-1}$ and hence these parameters were adopted although available lines were not particularly sensitive to the temperature. Temperature errors of $\pm 500 \text{ K}$ or more are possible. With these parameters the atmospheric chemical abundances for the central star are those reported in Table 13.

Table 13. Elemental Abundances for the central star of the PPN HDE 341617.

Species	$\log \epsilon_{\odot}$	[X/H]	s.d.	N
C II	8.55	-1.43		1
N II	7.97	-0.50	± 0.30	3
O II	8.87	-0.51	± 0.21	14
Mg II	7.58	-1.13		1
Si III	7.55	-0.63	± 0.06	2

Notes – same as Table 3.

6. Discussion

In order to estimate the mass and the age of each of the program stars we have plotted them on the H-R diagram as can be seen in Fig. 5. The effective temperatures are those derived from the chemical analysis, and the luminosities were obtained from the above temperatures and the calibration of Schmidt-Kaler (1982); these quantities are listed in Table 2. Despite parallaxes do exist in the Hipparchos catalogue for some of the stars in our sample, we have preferred the above approach for the luminosity calculation for the following reasons. While a very respected version of the Period - Luminosity relation for cepheids has been calculated using Hipparchos parallaxes (Feast & Catchpole 1997) using the most well-known 26 cepheids as calibrators, individual parallaxes seem to be of little use. We have taken 21 cepheids such that the distances could be estimated without requiring the use of paral-

axes. A straight comparison of distance moduli obtained from the Hipparchos parallaxes and from the P-L relation shows, in many cases, large differences. We have also noticed that Hipparchos parallaxes place some stars at unacceptable positions on the H-R diagram given the derived atmospheric parameters and elemental abundances. For example, for stars HD 172324 and HD 172481 the parallax data suggest values of $\log (L/L_{\odot}) < 2.7$. The situation is further complicated by unknown circumstellar reddening, which could be substantial for some of the stars, given their high infrared fluxes. Therefore we decided not to use individual parallaxes in the present context.

All pre-AGB evolutionary model tracks plotted in Fig. 5 are those of Schaller et al. (1992), while the post-AGB models are from Blöcker (1995). All isochrones are from the work of Bertelli et al. (1994).

In terms of evolution, we could distinguish three groups among our sample stars. First, HD 158616, HD 172324, HD 172481, and HDE 341617 show clear indications of being post-AGB stars, these are shown in panel *c* of Fig. 5. The post-AGB model sequences of Blöcker (1995) suggest that all four stars had initial ZAMS masses larger than $7 M_{\odot}$ and remnant or core mass of $\sim 1 M_{\odot}$. HD 158616 and HD 172481 might be starting their trajectory towards the white dwarfs region, i.e. they are near the zero age of central star evolution (Blöcker 1995), while HD 172324 is a bit more evolved. Since the evolution in this region of the H-R diagram is very fast, they are all expected to become planetary nebulae within a few hundreds of years. HDE 341617 has been found to be in the early stages of PN (Arkhipova et al. 1999; Parthasarathy et al. 2000). Our remnant mass estimate of $\sim 1 M_{\odot}$ is substantially larger than $0.7 M_{\odot}$ estimated by Arkhipova et al. (1999) from the rate of temperature evolutionary change and a comparison with the theoretical rates from Blöcker's (1995) models. Our value is a consequence of the spectroscopic determination of $T_{\text{eff}} = 23000 \text{ K}$ and hence $\log (L/L_{\odot}) = 4.6$ (Schmidt-Kaler 1982) as well as a comparison with the luminosities of Blöcker's (1995) models. While the Arkhipova et al.'s (1999) estimation is quite convincing the luminosity of the adopted model ($L/L_{\odot}) = 4.0$ seems too low as it would imply $T_{\text{eff}} \sim 18000 \text{ K}$ for bright giant star of luminosity class II. Such low a temperature is not supported by the detailed spectroscopic analyses. Thus an independent estimate of the luminosity seems necessary to settle the core mass of this star.

In the second evolutionary group we include the stars HD 725, HD 218753 and HD 331319. These are all moderately iron-deficient but otherwise show nearly solar abundances. The heliocentric radial velocities for HD 218753 and HD 331319 are small. They are most likely young massive disk supergiants or bright giants that have gone through some nuclear processing. This is suggested by the C depletion and Na enhancement, indicating the effect of CN processing and post first dredge-up stage. HD 725 is an interesting star since three Y II and one Ba II lines in-

icate mild enhancement of s -process elements. Since we count on very scarce number of lines of s -process elements, we can only say that the star shows signs of evolution beyond RGB.

The tracks and isochrones on Figs. 5a and 5b suggest $M \sim 1.5\text{--}2.0M_{\odot}$ and age of 7.9×10^8 yr for HD 218753 and $M \sim 11M_{\odot}$ and age of 2.2×10^7 yr for HD 331319. From tracks on Fig. 5b we estimate a mass of $M \leq 9M_{\odot}$ and age of 2.5×10^7 yr. Its rather large heliocentric radial velocity of -57 km s^{-1} calls for attention, however, a calculation of the galactocentric motion indicates that the star moves on the galactic plane and has a mildly eccentric galactic orbit. Its radial velocity could owe its origin to pulsations and/or orbital motions, although variability has not been reported.

The last two stars in our sample, HD 9167 and HD 173638, display, with few exceptions, solar abundances and no signs of nuclear processing. They are probably evolving very near the giant branch. The estimated masses and ages from Fig. 5b are respectively $M \sim 10M_{\odot}$ and 2.6×10^7 yr and $M \sim 12M_{\odot}$ and 1.7×10^7 yr. The only peculiarity of HD 9167 is its high radial velocity of -45.7 km s^{-1} however, like HD 725, its galactocentric orbit seems to be on the galactic plane and mildly eccentric. Also the possibility, that their observed radial velocities are attained from pulsation and/or orbital motion cannot be discarded.

It should be noted that although HD 172481 and HD 158616 are post-AGB stars, they do not show the effect of selective removal of condensable elements such as Fe and Sc, observed in some well-known post-AGB stars like HR 4049, and HD 52961 and RV Tau stars of subclass B (Giridhar, Lambert & Gonzalez 2000 and references therein). While studying a sample of RV Tau stars, these authors had noticed a strong dependence on temperature for the selective removal of refractory elements to occur. The effect is very prominent at temperature range 5500 to 6000 K and declines for lower temperatures. For stars cooler than 5000 K the effect was barely perceptible. At temperatures higher than 7000 K, we expect the effect to be larger. It is indeed true for HR 4049 (Lambert et al. 1988) which has $T_{\text{eff}} = 7500$ K, i.e. similar to HD 158616 and HD 172481. However, for these two stars we did not see any indication of dust condensation and subsequent removal of grain-forming elements. HD 158616 is a carbon-rich post-AGB star similar to HD 56126 (Klochova 1995) and HD 187785 (Van Winckel et al. 1996) also showing significant enhancement of s -process elements.

Stars like HR 4049, HD 52961 and RV Tau stars of subclass B show $C/O \leq 1$ and mild s -process enhancement. As a matter of fact, most stars showing abundance peculiarities caused by dust condensation have $C/O \leq 1$. Stars HR 4049, HD 44179, HD 46703, HD 52961 and BD +39° 4926 possibly belong to this subgroup. For these objects, since Fe gets locked in grains, $[S/H]$ is considered a better indicator of metallicity. For these stars $[S/H]$ ranges

between $+0.1$ to -1.0 dex with a mean around -0.4 dex. In other words, they are mildly metal-deficient. Carbon-rich post-AGB stars with enhanced s -process elements, like HD 158616, HD 56126 and HD 187785 have $[Fe/H]$ (which would be a true reflection of their metallicity since these stars are not affected by dust condensation) in the range -0.4 to -1.0 dex. These values are not radically different from those found for the subgroup having dust-grain condensation and $C/O \leq 1$. We, therefore, do not visualize large differences in their ages though the O-rich phase in the AGB is expected to precede the C-rich phase.

The abundances of hot post-AGB stars studied by Conlon et al. (1993a) and McCausland et al. (1992) bear close resemblance to HD 172324. The hot post-AGB stars show strong deficiency of carbon and significant oxygen enrichment. These stars probably belong to a subgroup of post-AGB star that have evolved without experiencing third dredge-up. This carbon deficiency is also found in the proto-Planetary Nebula HDE 341617 (see Table 13). Caution is however needed with C II spectra since they are known to show large non-LTE effects (Eber & Butler 1988; Takeda & Takada-Hidai 1994). McCausland et al. (1992) have discussed at length two scenarios to explain the carbon deficiency. HBB occurring during interpulse phase could cause the production of ^{14}N at the expense of ^{12}C . However, overabundance of He like the one found in the SMC planetary nebula SMP 28 is not evident for HD 172324 and HD 341617 to make HBB the sole mechanism responsible for carbon deficiency. Another possibility suggested by McCausland et al. (1992) that the carbon deficiency might be inherent to the precursor itself is quite attractive. To substantiate their argument they pointed out the carbon-poor stars HR 4912 and HR 7671 as possible precursors to more evolved carbon-poor hot post-AGB stars. HR 4912 was included in our recent work and we found $[C/H] = -1.27$ (Giridhar et al. 1997) in good agreement with $[C/H]$ of -1.15 found by Lambert, Luck & Bond (1983). HR 7671 has $[C/H]$ of -1.53 (Luck et al. 1990). It seems therefore that HD 172324 and HDE 341617 might form a special carbon-poor post-AGB stars evolutionary sequence. Search for carbon-poor objects in all temperature ranges may help in finding the precursors or successors of these objects.

7. Conclusions

We have found a new post-AGB star HD 172481 for which abundance analysis had not been carried out before, however the referee pointed out in a rather late stage of revision, the then unpublished work by Reyniers & Van Winckel (2001) where an independent abundance analysis has been carried out. We have highlighted a comparison of results in section 5.5 and found both analyses to be in fairly good agreement. We have done a more complete analysis of HD 158616. This star can be now considered a post-AGB star beyond any doubt. Among the

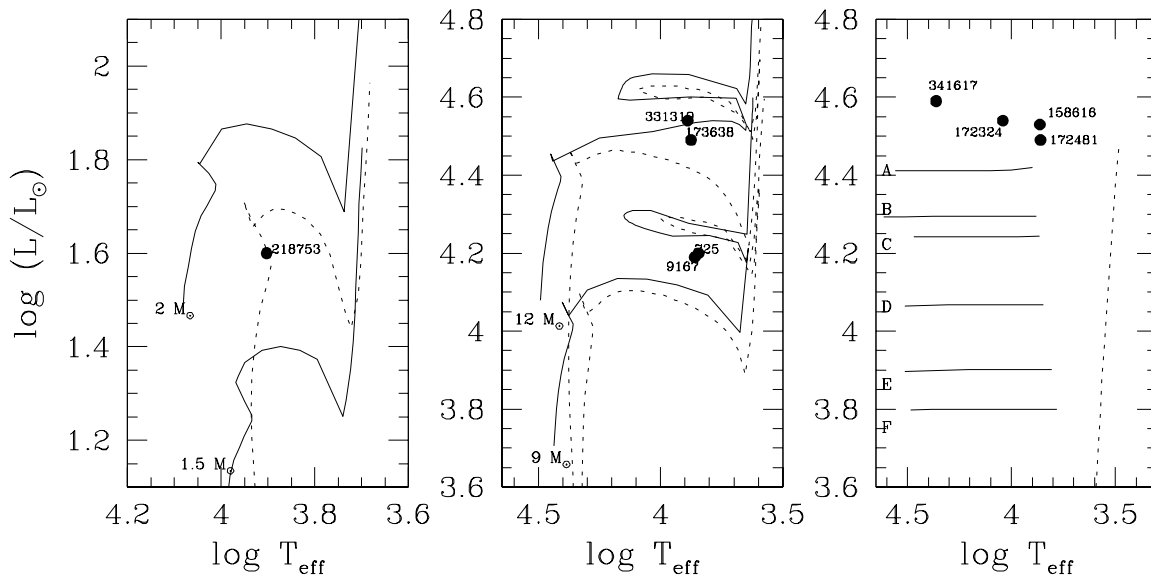


Fig. 5. H-R diagram showing the positions of sample stars along evolutionary tracks (continuous lines) and isochrones (dashed lines). T_{eff} and $\log(L/L_{\odot})$ are those in Table 2. The evolutionary tracks are from Schaller et al. (1992) and all isochrones from Bertelli et al. (1994). (a) The star HD 218753 has $M \sim 1.5 - 2.0M_{\odot}$ and age of 7.9×10^8 yr. (b) The two isochrones shown correspond to 3.16×10^7 and 2.0×10^7 yr. See text for discussion. (c) The post-AGB models are from Blöcker 1995 for ZAMS mass and core mass combinations ($M_{\text{zams}}, M_{\text{H}}$); A: = ($7M_{\odot}, 0.940M_{\odot}$), B: = ($3M_{\odot}, 0.836M_{\odot}$), C: = ($5M_{\odot}, 0.836M_{\odot}$), D: = ($4M_{\odot}, 0.696M_{\odot}$), E: = ($3M_{\odot}, 0.625M_{\odot}$), F: = ($3M_{\odot}, 0.605M_{\odot}$). The isochrone shown corresponds to 2.5×10^8 yr. See text for discussion.

post-AGB stars, the number of stars showing $C/O \sim 1$ or greater and also enhancement of s -process elements are very few. There are clear indications of stars having experienced the third dredge-up. The stars HD 158616 and HD 172481 belong to this important class. C/O of HD 172481 might have been prevented from exceeding one by HBB. The same may be responsible for large Li abundance but other possibilities like binarity cannot be ruled out. A long-term light and radial velocity monitoring of this object is planned for the future.

We found a very likely hot post-AGB candidate in HD 172324 but will feel more confident of its status after important elements like N are included and a more comprehensive study is made. Continuous monitoring of its spectrum in the H_{α} region is required to detect activity possibly related to stellar pulsations.

HD 218753 and HD 331319 have passed the giant branch and are in the He-core and H-shell burning stages. HD 9167 and HD 173638 essentially show solar abundance. HD 725 and HD 9167 show large radial velocities, however their galactocentric orbits are on the galactic plane and mildly eccentric, thus they are most likely massive and young disk stars. However, their large radial velocity could also be due to pulsations and/or orbital motions.

In the proto-Planetary Nebula HDE 341627 the He lines show two velocity components possibly indicating velocity stratification. The emission lines appear to have weakened since 1993.

Acknowledgements. AAF acknowledges Commission 38 of the IAU for a travel grant and the Indian Institute of Astrophysics for hospitality and financial support. We thank David Yong for getting us two spectra of HD 172481. We are also indebted to Ms. T. Sivarani for her help in identifying the lines for HDE 341617. We are grateful to the referee, Dr. R. Gallino, for helpful discussions and suggestions. This project has been supported at different stages by grants from DGAPA-UNAM (IN113599) and CONACyT (Mexico) (E130.2060) and CNRS (France).

References

- Arellano Ferro, A., 1985, *RMA&A* 11, 113
- Arellano Ferro, A., Giridhar, S., Goswami, A., 1991, *MNRAS* 250, 1
- Arellano Ferro, A., Mantegazza, L., 1996, *A&A* 315, 542
- Arhipova, V.P., Ikonnikova, N.P., Noskova, R.I., Sokol, G.V., Esipov, V.F., Klochkova, V.G., 1999, *Astronomy Letters* 25, 25
- Baranne, A., Queloz, D., Mayor, M., Adrianzyk, G., Knispel, G., Kohler, D., Lacroix, D., Meunier, J.-P., Rimbaud, G., Vin, A., 1996, *A&AS* 119, 373

- Bertelli, G., Bressan, A., Chiosi, C., Fagotto, F., Nasi, E., 1994, A&AS 106, 275
- Bidelman, W.P., 1990, in Luminous High-Latitude Stars, ASP Conf. Ser. 45, 47
- Blöcker, T., 1995, A&A 299, 755
- Bogart, E., 1994, Ph.D. Thesis, Katholieke Uni. Leuven.
- Bond, H.E., Luck, R.E., 1987, ApJ 312, 203
- Boothroyd, A.I., Sackmann, I.J., Ahern, S.C., 1993, ApJ 416, 762
- Boothroyd, A.I., Sackmann, I.J., 1999, ApJ 510, 232
- Boyarchuck, A.A., Lyubimkov, L.S., Sakhbullin, N.A., 1985, Astrophysics 22, 203
- Bravo Alfaro, H. Arellano Ferro, A., Schuster, W.J., 1997, PASP 109, 958
- Busso, M., Gallino, R., Wasserburg, G.J., 1999, ARA&A 37, 239
- Busso, M., Lambert, D.L., Beglio, L., Gallino, R., 1995, ApJ 446, 775
- Conlon, E.S., Dufton, P.L., McCausland, R.J.H., Keenan, F.P., 1993a, ApJ 408, 593
- Conlon, E.S., McCausland, R.J.H., Dufton, P.L., Keenan, F.P., 1993b, in Luminous High-Latitude Stars, ASP Conf. Ser. 45, 146
- Cowley, A., Cowley, Ch., Jaschek, M., Jaschek, C., 1969, AJ 74, 375
- Cramer, N., Maeder, A., 1979, A&A 78, 305
- Crawford, D., 1970, AJ 75, 624
- Crawford, D., 1979, AJ 84, 1858
- Decin, L., Van Winckel, H., Waelkens, C., Bakker, E.J., 1998, A&A 332, 928
- Didelon, P., 1982, A&AS 50, 199
- Downes, R.A., Keyes, C.D., 1988, AJ 96, 777
- Eber, F., Butler, K., 1988, A&A 202, 153
- Edvardsson, B., Andersen, J., Gustafsson, B., Lambert, D.L., Nissen, P.E., Tomkin, J., 1993, A&A 275, 101.
- Feast, M. W., Catchpole, R.M., 1997, MNRAS 286, L1
- Gallino, R., Arlandini, C., Busso, M., Lugaro, M., Travaglio, C., Straniero, O., Chieffi, A., Limongi, M., 1998, ApJ 497, 388
- Gigas, D., 1986 A&A 165, 170
- Giridhar, S., Arellano Ferro, A., 1989, JA&A 10, 47
- Giridhar, S., Arellano Ferro, A., 1995, RMA&A 31, 23
- Giridhar, S., Arellano Ferro, A., Parrao, L., 1997, PASP 109, 1077
- Giridhar, S., Lambert, D.L., Gonzalez, G., 2000, ApJ 531, 521
- Gonzalez, G., Lambert, D.L., Giridhar, S., 1997, ApJ 479, 427
- Grevesse, N., Noels, A., Sauval, A.J., 1996, ASP Conf. Ser. 99, 117
- Griffin, R. F. & Redman, R. O., 1960, MNRAS 120, 287
- Hauck, B., Mermilliod, M., 1998, A&AS 129, 431
- Klochkova, V.G., 1995, MNRAS 272, 710
- Kodaira, K., 1973, A&A 22, 273
- Kraft, P.R., Sneden, C., Langer, G.E., Prosser, C.F., 1992, AJ 104, 645
- Kurucz, R.L., (1993) ATLAS9 Stellar atmosphere Programs and 2km s⁻¹ grid CDROM Vol 13 (Cambridge: Smithsonian Astrophysical Observatory)
- Lambert, D.L., 1992, in Instabilities in Evolved Super and Hypergiants, ed. C. de Jager, H.Nieuwenhuijzen (Amsterdam: North-Holland), 156
- Lambert, D.L., Heath, J.E., Lemke, M., Drake, J., 1996, ApJS 103, 183
- Lambert, D.L., Hinkle, K.H., Luck, R.E., 1988, ApJ 333, 917
- Lambert, D.L., Luck, R.E., Bond, H.E., 1983, PASP 95, 413
- Langer, G.E., Hoffman, R., Sneden, C., 1993, PASP 105, 301
- Lattanzio, J.C., 1997, in 2nd Oak Ridge Symp. on Atomic and Nuclear Astrophysics, IOP Publishing Ltd.
- Luck, R.E., Bond, H.E., 1983, ApJ Lett. 271, L75
- Luck, R.E., Bond, H.E., 1984, ApJ 279, 729
- Luck, R.E., Bond, H.E., 1985, ApJ 292, 559
- Luck, R.E., Bond, H.E., Lambert, D.L., 1990, ApJ 357, 188
- McErlean, N.D., Lennon, D.J., Dufton, P.L., 1999, A&A 349, 553
- McCarthy, J.K., Sandiford, B.A., Boyd, D., Booth, J., 1993, PASP 105, 881
- McCausland, R.J.H., Conlon, E.S., Dufton, P.L., Keenan, F.P., 1992, ApJ 394, 298
- Morgan, W. W., Roman, N. G., 1950, ApJ 112, 362
- Mowlavi, N., 1999, New Astr. Rev. 43, 389
- Napiwotzki, R., Schönberner, D., Wenske, V., 1993, A&A 268, 653
- Olsen, E.H., A&AS 1983, 54, 55
- Olson, F.M., Baud, B., Habing, H.J., de Jong, T., Harris, S., Pottasch, S.R., 1984, ApJL 278, L41
- Parthasarathy, M., García-Lario, P., Sivarani, T., Manchado, A., Sanz Fernandez de Córdoba, L., A&A 2000, 357, 241.
- Perry, C.L., AJ 1969, 74, 705
- Reddy, B.E., 1996, Ph D. Thesis, Bangalore University, India.
- Reyniers, M., Van Winckel, H., 2001, A&A in press.
- Sackmann, I.J., Boothroyd, A.I., 1992, ApJ 392, L71.
- Schaller, G., Schaerer, D., Meynet, G., Maeder, A., 1992, A&AS 96, 269
- Schmidt-Kaler, Th., 1982, in *Numerical Data and Functional Relationships in Science and Technology*, eds. K. Schaifers and H.H. Vogt. Springer-Verlag.
- Schwarzschild, M., Härm, R., 1965, ApJ 142, 885
- Smith, V.V., Plez, B., Lambert, D.L., 1995, ApJ 441, 735
- Sneden, C., 1973, Ph.D. Thesis, Univ. of Texas at Austin
- Sneden, C., Kraft, R.P., Prosser, C.F., Langer, G.E., 1991, AJ 102, 2001
- Stephenson, C.B., 1986, ApJ 300, 779
- Straniero, O., Chieffi, A., Limongi, M., Busso, M., Gallino, R., Arlandini, C., 1997, ApJ 478, 332
- Straniero, O., Gallino, R., Busso, M., Chieffi, A., Raiteri, C.M., 1995, ApJ 440, L85
- Takeda, Y., Takada-Hidai, M., 1994, PASJ 46, 395
- Takeda, Y., Takada-Hidai, M., Kotake, J., 1996, PASJ 48, 753
- Takeda, Y., Takada-Hidai, M., 1998, PASJ 50, 629
- Thévenin, F., 1989, A&AS 77, 137
- Thévenin, F., 1990, A&AS 82, 179
- Travaglio, C., Galli, D., Gallino, R., Busso, M., Ferrini, F., Straniero, O., 1999, ApJ 521, 691
- Tull, R.G., MacQueen, P.J., Sneden, C., Lambert, D.L., 1995, PASP 107, 251.
- van der Veen, W. and Habing, H.J., 1988, A&A 194, 125
- Van Winckel, H., 1995, Ph.D. Thesis, Katholieke Univ. Leuven, Netherlands.
- Van Winckel, H., 1997, A&A 319, 561
- Van Winckel, H., Reyniers, M., 2000, A&A 354, 135
- Van Winckel, H., Waelkens, Ch., Waters, L.B.F.M., 1996, A&A 306, L37

- Venn, K.A., 1995a, ApJS 99, 659
 Venn, K.A., 1995b, ApJ 449, 832
 Volk, K.M., Kwok, S., 1989, ApJ 342, 345
 Wallerstein, G., Iben, I.Jr, Parker, P., Boesgaard, A.M., Hale, G.M., et al., 1997, Rev. Mod. Phys. 69, 995
 Weigert, A., 1966, Z. Astrophys. 64, 395
 Wiese, W.L., Fühner, J.R., Deters, T.M., 1996, Jour. of Phy. and Chem. ref. data Monograph No. 7
 Wheeler, J. C., Sneden, Ch., Truran, J. W., 1989, ARA&A 27, 279

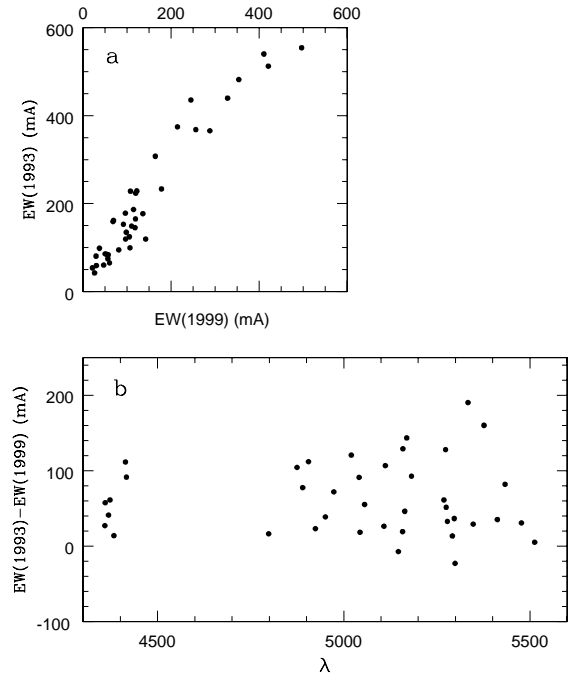


Fig. 4. A comparison of equivalent widths of the emission spectrum of HDE 341617 as observed in 1993 and in 1999. (a) The weakening of the emission spectrum is evident despite the fact that the 1999 spectra have not been flux calibrated. (b) The equivalent widths are not a function of wavelength. However, the large scatter is probably due to the lack of calibration. See text for discussion.

Table 11. Absorption lines in the spectrum of the proto-Planetary Nebula HDE 341617

Species	λ_{obs} (\AA)	λ_{lab} (\AA)	$Eq.W.$ ($m \text{\AA}$)	Vr ($km s^{-1}$)	Species	λ_{obs} (\AA)	λ_{lab} (\AA)	$Eq.W.$ ($m \text{\AA}$)	Vr ($km s^{-1}$)
He I	4010.217	4009.270	223.2	70.9	O II	4642.973	4641.811	233.6	75.1
He I	4027.047	4026.362	337.0	48.6	O II	4643.039	4641.82	302.9	78.8
He I	4144.569	4143.759	391.9	51.0	O II	4650.29	4649.139	309.0	74.3
O II:	4350.53	4349.426	267.7	76.1	O II	4662.795	4661.635	150.4	74.7
O II	4367.922	4366.896	208.3	70.5	O II+C III	4674.776	4673.91/73.75	58.6	
He I	4389.027	4387.929	325.8	75.1	O II	4677.389	4676.234	84.8	74.1
O II	4415.984	4414.909	141.5	73.0	O II	4706.507	4705.355	70.2	73.4
O II	4418.081	4416.975	104.7	75.1	He I	4714.39	4713.143	160.8	79.4
He I	4472.59	4471.477	446.8	74.7	He I	4922.992	4921.929	516.4	64.8
Si III	4553.727	4552.654	322.4	70.7	He I:	5015.647	5015.675	217.2	
Si III	4568.918	4567.872	280.0	68.7	Fe II	5796.901	5795.870	152.8	53.4
Si III	4575.818	4574.777	229.7	68.3	He I bld	5875.849	5875.618+75.650	542.5	
O II	4592.136	4590.971	209.9	76.1	He I	6679.176	6678.149	841.9	46.1
O II	4639.951	4638.854	136.3	70.9					

Table 12. Emission lines in the spectrum of the proto-Planetary Nebula HDE 341617

Species	λ_{obs} (\AA)	λ_{lab} (\AA)	$Eq.W.$ ($m \text{\AA}$)	Vr ($km s^{-1}$)	Species	λ_{obs} (\AA)	λ_{lab} (\AA)	$Eq.W.$ ($m \text{\AA}$)	Vr ($km s^{-1}$)
[S II]	4069.357	4068.600	545.7	55.8	[Cr I:]	5147.604	5146.550	86.5	61.4
[Fe II]	4244.732	4243.980	266.3	53.1	[Fe II]	5158.931	5158.000	155.2	54.1
[Fe II]	4245.566	4244.810	50.0	53.4	[Fe II]	5159.702	5158.810	367.9	51.8
[Fe II]	4277.632	4276.83	237.5	56.2	[Fe II]	5164.910	5163.940	108.9	56.4
[Fe II]	4306.718	4305.900	60.2	57.0	Fe II	5169.933	5169.030	164.1	52.4
H γ	4341.315	4340.475	1030.0		[Fe II]	5182.956	5181.970	89.0	57.1
[Fe II]	4353.553	4352.78	100.5	58.8	[Fe II]	5200.056	5199.180	43.0	50.5
[Fe II]	4359.146	4358.370	117.9	53.4	[Fe II]	5221.008	5220.060	74.3	54.5
[Fe II]	4360.112	4359.190	496.6	53.1	[Fe II]	5262.580	5261.610	463.8	55.3
O I	4369.018	4368.30	100.9	49.3	[Fe II]	5269.799	5268.880	58.5	52.3
Fe II	4373.130	4372.220	37.1	62.4	[Fe II]	4288.157	4287.40	625.2	53.0
[Fe II]	4383.621	4382.750	81.0	59.6	[Fe II]	5274.345	5273.380	383.7	54.9
Fe II	4385.381	4384.330	24.7	71.9	O I	5276.020	5275.080	29.2	53.5
[Fe II]	4414.564	4413.780	398.2	53.3	Fe II	5279.221	5278.265	21.1	54.3
[Fe II]	4417.075	4416.270	356.9	54.7	Fe III	5292.588	5291.780	46.7	45.0
[FeII]	4458.737	4457.95	221	52.9	[Fe II]	5297.799	5296.840	78.1	54.3
[Fe II]	5413.604	5412.640	50.3	53.4	O I	5299.961	5299.000	117.2	54.4
[FeII]	4475.767	4474.91	85	53.0	Fe II	5317.554	5316.609	23.9	53.3
[FeII]	4489.560	4488.75	85	51.0	[Fe II]	5334.587	5333.650	295.0	52.7
[FeII]	4493.412	4492.64	38	53.4	[Fe II]	5348.652	5347.690	30.0	54.0
[FeII]	4529.249	4528.39	18	56.4	[Fe II]	5377.438	5376.470	234.3	54.0
[FeII]	4728.955	4728.07	170	56.4	[Fe II]	5434.124	5433.150	86.1	53.8
Fe III	4734.765	4733.900	14.9	54.8	[Fe II]	5478.195	5477.250	43.9	51.8
[FeII]	4775.615	4774.74	110	54.4	O I	5513.699	5512.710	30.0	53.8
[Fe II]	4799.149	4798.29	25.9	53.7	O I	5555.937	5554.940	60.0	53.8
[Fe II]	4815.394	4814.5	325.9	52.8	[Fe II]	5747.997	5746.960	130.2	54.1
H β	4862.284	4861.332	2921.0	58.7	[N II]	5755.637	5754.800	157.5	43.6
[Fe II]	4875.354	4874.490	116.5	53.2	Si II	5958.641	5957.612	149.5	51.8
[Fe II]	4890.511	4889.630	288.0	54.1	O I	5959.607	5958.46+58.630		
[Fe II]	4906.204	4905.350	256.0	52.2	Si II o FeIII	5979.989	5978.970	425.3	51.1
Fe II	4924.813	4923.921	86.3	54.3	O I bld	6047.481	6046.26+6046.46	427.2	60.6
[Fe II]	4951.656	4950.740	46.0	55.5	Si II(2)+[NII]	6348.259	6347.090	517.8	55.3
[Fe II]	4974.283	4973.390	101.5	53.9	[O I]	6364.896	6363.88	277.7	47.9
uf ¹	4981.034		113.5		uf ¹	6366.259		126.3	
[Fe II]	5006.441	5005.520	69.1	43.2	Si II(2)	6372.505	6371.359	242.9	54.0
Fe II	5019.322	5018.434	97.5	53.17	[N II](1)	6549.274	6548.100	666.1	53.8
[Fe II]	5021.110	5020.240	107.4	52.0	H α	6564.138	6562.817	43.97	60.3
Si II	5041.962	5041.063	61.9	53.5	[N II](1)	6584.646	6583.6	2105.0	47.7
[Fe II]	5044.422	5043.530	58.1	53.1	[O II]	6668.000	6666.940	160.2	47.
Si II	5056.882	5056.020	178.0	51.1	[S II]	6717.786	6716.470	81.1	58.8
[Fe II]	5108.814	5107.950	57.1	50.7	[S II]	6731.874	6730.850	93.3	45.6
[Fe II]	5112.558	5111.630	88.8	54.5	[S II]	6732.169	6731.300	114.5	38.72

1 – uf = unidentified feature.

Table 14. Comparison of relevant [X/Fe] ratios for program stars and well known post-AGB stars.

Star	[Fe/H]	[C/Fe]	[O/Fe]	[Mg/Fe]	[Si/Fe]	[S/Fe]	[Ca/Fe]	[s/Fe]	C/O	reference
HD 725	-0.29	-0.08		+0.12	+0.40	+0.20	+0.14	+0.27		1
HD 9167	-0.34			-0.04			+0.12	+0.12		1
HD 172324	-0.63	-0.68	+0.96	-0.02	+0.43	+0.42			+0.01	1
HD 173638	-0.08	-0.09		+0.03	+0.46		+0.09	+0.14		1
HD 218753	-0.19	-0.30	+0.05	-0.09	+0.23	+0.36	+0.11	+0.14	+0.21	1
HD 331319	-0.24	-0.09	+0.30	-0.01	+0.06	+0.53	-0.05	-0.30	+0.19	1
HD 158616	-0.57	+0.34	+0.04	+0.08	+0.56	+0.62	+0.21	+0.66	+0.95	1
HD 158616	-0.70	+0.64	-0.04		+0.68	+0.70	+0.71	+1.30	+1.90	2
HD 172481	-0.61	-0.01	+0.04	+0.51	+0.54	+0.58	+0.34	+0.52	+0.43	1
HR 7671	-1.10	-0.40	-0.30	+0.25	+0.40	+0.15	+0.32	+0.60	+0.38	6
HD 187785	-0.40	+1.00	+0.60	+0.67	+0.82	+0.57	+0.49	+1.30	+1.20	4
HD 187785	-0.60	+1.00	+0.70	+0.38		+0.26	+0.49	+1.10		11
HD 56126	-1.00	+1.08	+0.63	+0.97	+0.95	+0.63	+0.46	+1.78	+1.35	3
HD 56126	-1.00	+1.10	+0.80	+0.06		+0.40	-0.11	+1.50		11
IRAS04296+3429	-0.60	+0.80			+0.79	+0.43	+0.18	+1.50		11
IRAS05341+0852	-0.80	+1.00	+0.60		+0.59	+0.28	+0.08	+2.20		11
IRAS22223+4237	-0.30	+0.30	-0.10		+0.29	+0.04	-0.17	+0.90		11
IRAS23304+6147	-0.80	+0.90	+0.20		+0.79	+0.56	+0.29	+1.60		11
HR 4049	< -3.2	> +3.0	> +2.7	> +1.7	> +0.40	> +3.0	< -2.1		+0.95	5
HD 44179	-3.30	+3.30	+2.90	+1.2	+1.50	+3.00		+0.20	+1.20	2
HD 46703	-1.57	+0.98	+1.10	+0.09	-0.38	+1.20	+0.02	-0.49	+0.74	7,8
HD 52961	-4.80	+4.40	+4.20			+3.80		+0.60	+0.76	2
HD 70379	-0.31	+0.42	+0.38	+0.01	+0.47	+0.34	-0.17	+0.20	+0.47	9
BD+39 4926	-2.85	+2.45	+2.75	+1.35	+1.15	+2.95	-0.75	+1.60	+0.25	10

References: 1 – This work, 2 – Van Winckel (1995) , 3 –Klochkova (1995), 4 – Van Winckel et al. (1996), 5 – Lambert et al. (1988), 6 – Luck et al. (1990), 7 – Luck & Bond (1984), 8 – Bond & Luck (1987), 9 – Reddy (1996), 10 – Kodaira (1973), 11 – Van Winckel & Reyniers (2000).